

# Comparing the Robustness of Modern No-Reference Image- and Video-Quality Metrics to Adversarial Attacks

Anastasia Antsiferova<sup>1,2</sup>, Khaled Abud<sup>3</sup>, Aleksandr Gushchin<sup>1,2,3</sup>, Ekaterina Shumitskaya<sup>3</sup>, Sergey Lavrushkin<sup>1,2</sup>, Dmitriy Vatolin<sup>1,2,3</sup>

<sup>1</sup>MSU Institute for Artificial Intelligence

<sup>2</sup>ISP RAS Research Center for Trusted Artificial Intelligence

<sup>3</sup>Lomonosov Moscow State University

{aantsiferova, khaled.abud, alexander.gushchin, ekaterina.shumitskaya, sergey.lavrushkin, dmitriy}@graphics.cs.msu.ru

## Abstract

Nowadays, neural-network-based image- and video-quality metrics perform better than traditional methods. However, they also became more vulnerable to adversarial attacks that increase metrics' scores without improving visual quality. The existing benchmarks of quality metrics compare their performance in terms of correlation with subjective quality and calculation time. Nonetheless, the adversarial robustness of image-quality metrics is also an area worth researching. This paper analyses modern metrics' robustness to different adversarial attacks. We adapted adversarial attacks from computer vision tasks and compared attacks' efficiency against 15 no-reference image- and video-quality metrics. Some metrics showed high resistance to adversarial attacks, which makes their usage in benchmarks safer than vulnerable metrics. The benchmark accepts submissions of new metrics for researchers who want to make their metrics more robust to attacks or to find such metrics for their needs. The latest results can be found online: <https://videoprocessing.ai/benchmarks/metrics-robustness.html>.

## Introduction

Nowadays, most new image- and video-quality metrics (IQA/VQA) employ deep learning. For example, in the latest NTIRE challenge on perceptual quality assessment (Gu et al. 2022), all winning methods were based on neural networks. With the increased sizes of datasets and availability of crowdsourced markup, deep-learning-based metrics started to outperform traditional approaches in correlation with subjective quality. However, learning-based methods, including IQA/VQA metrics, are more vulnerable to adversarial attacks. A simple metric like PSNR is more stable to image modifications that aim to manipulate quality scores (any changed pixel will decrease the score). In contrast, the behaviour of deep metrics is much more complex. The existing benchmarks evaluate metrics' correlation with subjective quality but do not consider their robustness. At the same time, *the possibility to manipulate IQA/VQA metrics scores is already being exploited in different real-life scenarios*. Below are some examples of such scenarios and potential negative impacts from using non-robust IQA/VQA.

*Decrease of perceptual quality.* Metrics-oriented optimization modes are already being implemented in video encoders. libaom (Deng, Han, and Xu 2020) and LCEVC (V-Nova 2023) have options that optimize bitstream for increasing a VMAF score. Such tuning was designed to improve the visual quality of the encoded video; however, as VMAF is a learning-based metric, it may decrease perceptual quality (Zvezdakova et al. 2019; Siniukov et al. 2021). Using unstable image quality metrics as a perceptual proxy in a loss function may lead to incorrect restoration results (Ding et al. 2021). For instance, LPIPS is widely used as a perceptual metric, but optimizing its scores leads to increased brightness (Kettunen, Härkönen, and Lehtinen 2019), which is unwanted or even harmful (for example, when analyzing medical images).

*Cheating in benchmarks.* The developers of image- and video-processing methods can use metrics' vulnerabilities to achieve better competition results. For example, despite LPIPS already being shown to be vulnerable to adversarial attacks, it is still used as the main metric in some benchmarks, e.g. to compare super-resolution methods (Zhang et al. 2021). In some competitions that publish the results of subjective comparisons and objective quality scores, we can see the vast difference in these leaderboards. For instance, the VMAF leaders in 2021 Subjective Video Codecs Comparisons differ from leaders by subjective quality (Comparison 2021).

*Manipulating the results of image web search.* Search engines use not only keywords and descriptions but also image quality measurement to rank image search results. For example, the developers of Microsoft Bing used image quality as one of the features to improve its output (Bing 2013). As shown in MediaEval 2020 Pixel Privacy: Quality Camouflage for Social Images competition (MediaEval 2020), there are a variety of ways to fool image quality estimators.

Our study highlights the necessity of measuring the adversarial robustness of contemporary metrics for the research community. There are different ways to cheat on IQA/VQA metrics, such as increasing or decreasing their scores. In our study, we focus on analyzing metrics' resistance to attacks that increase estimated quality scores, as this kind of attack has already appeared in many real-life cases. Also, by choosing to investigate metrics' stability to scores increasing, we do not limit the generability of the results. We believe that

the existing image- and video-quality metrics benchmarks must be supplemented with metrics’ robustness analysis. In this paper, we first attempt to do this and apply several types of adversarial attacks to a number of quality metrics. Our contributions are as follows: a new benchmark methodology, a leaderboard published online <sup>1</sup>, and an analysis of currently obtained results. We published our code <sup>2</sup> for generating adversarial attacks and a list of open datasets used in this study, so the developers of IQA/VQA methods can measure the stability of their methods to attacks. For those who want their approach published on our website, the benchmark accepts new submissions of quality metrics. Try our benchmark using *pip install robustness-benchmark*.

## Related Work

Depending on the availability of the undistorted image, IQA/VQA metrics can be divided into three types: no-reference (NR), full-reference (FR) or reduced-reference (RR). NR metrics have the broadest applications but generally show lower correlations with subjective quality than FR and RR metrics. However, recent results show that new NR metrics outperformed many existing FR methods, so we mainly focused on NR metric evaluation in this paper. The performance of IQA/VQA metrics is traditionally evaluated using subjective tests that measure the correlation of metric scores with perceptual ones. The most well-known comparisons were published within NTIRE Workshop (Gu et al. 2022), and two benchmarks currently accept new submissions: MSU Video Quality Metrics Benchmark (Antsiferova et al. 2022) and UGC-VQA (Tu et al. 2021). These studies show how well the compared metrics estimate subjective quality but do not reflect their robustness to adversarial attacks.

There are different ways to measure the robustness of neural network-based methods. It can be done via theoretical estimations, e.g. Lipschitz regularity. However, this approach has many limitations, including the number of parameters in the evaluated network. A more universal approach is based on applying adversarial attacks. This area is widely studied for computer vision models. However, not all methods can be adapted to attack quality metrics.

The first methods for measuring the robustness of IQA/VQA metrics were based on creating a specific situation in which the metric potentially fails. Ciaramello and Reibman (2011a) first conducted such analysis and proposed a method to reveal the potential vulnerabilities of an objective quality model based on the generation of image or video pairs with the intent to cause misclassification errors (Brill et al. 2004) by this model. Misclassification errors include false ordering (FO, the objective model rates a pair opposite to humans), false differentiation (FD, the objective model rates a pair as different but humans do not), and false tie (FT, humans order a pair as different, but the objective model does not). H. Liu and A. Reibman (2016) introduced a soft-

<sup>1</sup><https://videoprocessing.ai/benchmarks/metrics-robustness.html>

<sup>2</sup>[https://github.com/msu-video-group/MSU\\_Metrics\\_Robustness\\_Benchmark](https://github.com/msu-video-group/MSU_Metrics_Robustness_Benchmark)

Benchmark	# attacks / # metrics	Metrics type	Test datasets
Ciaramello and Reibman (2011a)	5 / 4	FR	10 images
Ciaramello and Reibman (2011b)	5 / 9	NR, FR	473 images
Liu and Reibman (2016)	5 / 11	NR, FR	60 images
Shumitskaya et al. (2022)	1 / 7	NR	20 videos
Zhang et al. (2022)	1 / 4	NR	12 images
Ghildyal and Liu (2023)	6 / 5	FR	12,227 images
Ours	9 / 15	NR, FR	3000 images, 1 video

Table 1: Comparisons of image- and video-quality metrics’ stability to adversarial attacks.

ware called “STIQE” that automatically explores an image-quality metric’s performance. It allows users to execute tests and then generate reports to determine how well the metric performs. Testing consists of applying several varying distortions to images and checking whether the metric score rises monotonically as the degree of the applied distortion.

Nowadays, metrics’ adversarial robustness is primarily estimated by adapting attacks designed for computer vision tasks to image quality metrics. A more detailed description of existing attacks against metrics that we used in our study is given in the section “List of adversarial attacks”. There are two recently published attacks that we aim to add to the benchmark shortly: a new CNN-based generative attack FACPA (Shumitskaya, Antsiferova, and Vatolin 2023), attack with human-in-the-loop by Zhang et al. (Zhang et al. 2022) and spatial attack that was adapted for metrics (Ghildyal and Liu 2023).

Recently, a new study on the adversarial robustness of full-reference metrics was published (Ghildyal and Liu 2023). The authors showed that six full-reference metrics are susceptible to imperceptible perturbations generated via common adversarial attacks such as FGSM (Goodfellow, Shlens, and Szegedy 2015), PGD (Madry et al. 2017), and the One-pixel attack (Su, Vargas, and Sakurai 2019). They also showed that adversarial perturbations crafted for LPIPS metric (Zhang et al. 2018) using stAdv attack can be transferred to other metrics. As a result, they concluded that more accurate learning-based metrics are less robust to adversarial attacks than traditional ones. We summarised the existing research on IQA/VQA metrics’ robustness to adversarial attacks in Table 1.

## Benchmark

### List of Metrics

In this paper, we focused on the evaluation of only no-reference metrics for several reasons: firstly, there exists a similar evaluation of full-reference metrics (Ghildyal and

Liu 2023); secondly, no-reference metrics have a more comprehensive range of applications and are more vulnerable to attacks; thirdly, these metrics are mostly learning-based. We considered state-of-the-art metrics according to other benchmarks and various other no-reference metrics. All tested metrics assess image quality, except for VSFA (Li, Jiang, and Jiang 2019) and MDTVSFA (Li, Jiang, and Jiang 2021), which are designed for videos.

**RankIQ**A (Liu, Van De Weijer, and Bagdanov 2017) pre-trains a model on a large dataset with synthetic distortions to compare pairs of images, then fine-tunes it on a small realistic dataset. **MetaIQ**A (Zhu et al. 2020) introduces a quality prior model pre-trained on several dozens of specific distortions and fine-tuned on a smaller target dataset, similar to RankIQ. **WSP** (Su and Korhonen 2020) is concerned with Global Average Pooling feature aggregation used by most existing methods and replaces it with Weighted Spatial Pooling to distinguish important locations. **CLIP-IQA** (Wang, Chan, and Loy 2023) predicts the quality perception and image-provoked abstract emotions by feeding heterogeneous text prompts and the image to the CLIP network. **PAQ-2-PIQ** (Ying et al. 2020) introduces a large subjective picture quality database of about 40,000 images, trains a CNN with ResNet-18 backbone to predict patch quality and combines the predictions with RoI pooling. **HyperIQ**A (Su et al. 2020) focuses on real-life IQA and proposes a hyper-convolutional network that predicts the weights of fully connected layers. **MANIQ**A (Yang et al. 2022) assesses quality of GAN-based distortions. The model uses vision transformer features processed by proposed network modules to enhance global and local interactions. The final score prediction utilizes patch weighting. **TReS** (Golestaneh, Dadsetan, and Kitani 2022) proposes to compute local features with CNN and non-local features with self-attention, introduces a per-batch loss for correct ranking and a self-supervision loss between reference and flipped images. **FPR** (Chen et al. 2022) hallucinates pseudo-reference features from the distorted image using mutual learning on reference and distorted images with triplet loss. Attention maps are predicted to aggregate scores over patches. **VSFA** (Li, Jiang, and Jiang 2019) estimates video quality using ResNet-50 features for content awareness and differentiable temporal aggregation, which consists of gated recurrent units with min pooling. **MDTVSFA** (Li, Jiang, and Jiang 2021) enhances VSFA with explicit mapping between predicted and dataset-specific scores, supported by multi-dataset training. **NIMA** (Talebi and Milanfar 2018) predicts a distribution of scores instead of regressing a single value and considers both technical and aesthetic image scores. It is trained on the Aesthetic Visual Analysis database using squared earth mover’s distance as a loss. **LINEARITY** (Li, Jiang, and Jiang 2020) invents the norm-in-norm loss, which shows ten times faster convergence than MSE or MAE with ResNet architecture. **SPAQ** (Fang et al. 2020) collects a database of 11,125 smartphone photos, proposes a ResNet-50 baseline model and three modified versions incorporating EXIF data (MT-E), subjective image attributes (MT-A) and scene labels (MT-S). **KonCept512** (Hosu et al. 2020) collects KonIQ-10k, a diverse crowdsourced database of 10,073 images and trains

a model with InceptionResNetV2 backbone.

We also used MSE, PSNR and SSIM (Wang et al. 2004) as proxy metrics to estimate image quality degradation after attacks. The choice is motivated by their structure (full-reference and not learning-based), which makes them more stable to adversarial attacks.

## List of Adversarial Attacks

In all attacks, we define the loss function as  $J(\theta, I) = 1 - score(I)/range$  and minimize it by making small steps along the gradient direction in image space, which increases the attacked metric score.  $range$  is computed as the difference between maximum and minimum metric values on the dataset and serves to normalize the gradient magnitude across different metrics.

**FGSM-based attacks** are performed for each image. The pixel difference is limited by  $\varepsilon$ . **FGSM** (Goodfellow, Shlens, and Szegedy 2015) is a basic approach that makes one gradient step:  $I^{adv} = I - \varepsilon \cdot sign(\nabla_I J(\theta, I))$ . **I-FGSM** (Kurakin, Goodfellow, and Bengio 2018) is a more computationally expensive method that uses  $T$  iterations and clips the image on each step:  $I_{t+1}^{adv} = Clip_{I, \varepsilon}\{I_t^{adv} - \alpha \cdot sign(\nabla_I J(\theta, I_t^{adv}))\}$ , where  $t = 0, 1, \dots, T - 1$ ,  $I_0$  is the input image  $I$ , and  $\alpha$  is the perturbation intensity. The clipped pixel value at position  $(x, y)$  and channel  $c$  satisfies  $|I_t^{adv}(x, y, c) - I(x, y, c)| < \varepsilon$ . **PGD** (Madry et al. 2017) is identical to I-FGSM except for the random initialization in the  $\varepsilon$ -vicinity of the original image; due to its similarity to I-FGSM, we didn’t include it in the experiments. **MI-FGSM** (Dong et al. 2018) uses gradient momentum:  $I_{t+1}^{adv} = Clip_{I, \varepsilon}\{I_t^{adv} - \alpha \cdot sign(g_t)\}$ ,  $t = 0, 1, \dots, T - 1$ ,  $g_t = \nabla_I J(\theta, I_t^{adv}) + \nu \cdot g_{t-1}$ ,  $g_{-1} = 0$ , where  $\nu$  controls the momentum preservation. **AMI-FGSM** (Sang et al. 2022) is identical to MI-FGSM, except the pixel difference limit  $\varepsilon$  is set to  $1/NIQE(I)$  by computing the NIQE (Mittal, Soundararajan, and Bovik 2012) no-reference metric.

**Universal Adversarial Perturbation (UAP)-based attacks** generate adversarial perturbation for an attacked metric, which is the same for all images and videos. When UAP is generated, the attack process consists of the mere addition of an image with UAP. The outcome is the image with an increased target metric score. We used three methods to train UAPs. **Cumulative-UAP** is obtained by averaging non-universal perturbation on the training dataset. Non-universal perturbations are generated using one step of gradient descent. **Optimized-UAP** is obtained by training UAP weights using batch training with Adam optimizer and loss function defined as target metric with opposite sign. **Generative-UAP** is obtained by auxiliary U-Net generator training. The network is trained to generate a UAP from random noise with uniform distribution. The Adam optimizer is used for training, and the loss function is defined as the target metric with the opposite sign. Once the network is trained, a generated UAP is saved and further used to attack new images.

**Perceptual-aware attacks** use other image quality metrics to control attack imperceptibility to the human eye. **Korhonen et al.** (Korhonen and You 2022) proposes a method for generating adversarial images for NR quality metrics

with perturbations located in textured regions. They use gradient descent with additional elementwise multiplication of gradients by a spatial activity map. The spatial activity map of an image is calculated using horizontal and vertical  $3 \times 3$  Sobel filters. **MADC** (Wang and Simoncelli 2008) is a method for comparing two image- or video-quality metrics by constructing a pair of examples that maximize or minimize the score of one metric while keeping the other fixed. In our study, we fixed MSE while maximizing an attacked metric. The projected gradient descent step and binary search are performed on each iteration. Let  $g_1$  be the gradient with direction to increase the attacked metric and  $g_2$  the gradient of MSE on some iteration. The projected gradient is then calculated as  $pg = g_1 - \frac{g_2^T \cdot g_1}{g_2^T \cdot g_2} \cdot g_2$ . After projected gradient descent, the binary search to guarantee a fixed MSE is performed (with 0.04 precision). The binary search is the process that consists of small steps along the MSE gradient: if the precision is bigger than 0.04, then steps are taken along the direction of reducing MSE and vice versa.

## Methodology

**Datasets** This study incorporated pre-trained quality metrics as a part of our evaluation benchmark. We did not perform metrics fine-tuning on any data. We used six datasets summarised in Table 2. These datasets are widely used in the computer vision field. We chose them to cover a diverse range of real-life scenarios, including images and video, with varying resolutions from  $299 \times 299$  up to  $1920 \times 1080$  (FullHD). All datasets have an open license that allows them to be used in this work. Our analysis categorized the adversarial attacks into trainable and non-trainable attacks. Three datasets were used to train adversarial attacks, and three were used for testing. We trained UAP attacks using each training dataset, resulting in three versions of each attack. These versions were subsequently evaluated on the designated testing datasets, and the results for different versions were averaged among each UAP-attack type and amplitude. Non-trainable attacks were directly evaluated on the testing datasets. We have analyzed the efficiency and generalization capabilities of both trainable and non-trainable adversarial attacks across various data domains while also considering the influence of training data on metric robustness. NIPS 2017: Adversarial Learning Development Set (2017) was also used to train metrics’ domain transformations (described further in “Evaluation metrics”).

**Implementation Details** We used public source code for all metrics without additional pretraining and selected the default parameters to avoid overfitting. The training and evaluation of attacks on the metrics were fully automated. We employed the CI/CD tools within a GitLab repository for our measurement procedures. We established a sophisticated end-to-end pipeline from the attacked metrics’ original repositories to the resulting robustness scores to make the results entirely verifiable and reproducible. The pipeline scheme, the list of used attack’s hyper-parameters and the hyperparameter choice justification are presented in the supplementary materials (Antsiferova et al. 2023). UAP-based attacks (UAP, cumulative UAP and generative UAP) were

averaged with three different amplitudes (0.2, 0.4 and 0.8).

Quality metrics implementations were obtained from official repositories. We only modified interfaces to meet our requirements and used default parameters provided by the authors. Links to original repositories and a list of applied patches (where it was needed to enable gradients) are provided in supplementary materials (Antsiferova et al. 2023).

Calculations were performed on two computers with the following characteristics:

- 4 x GeForce RTX 3090 GPU, an Intel(R) Xeon(R) Gold 6226R CPU @ 2.90GHz
- 4 x NVIDIA RTX A6000 GPU, AMD EPYC 7532 32-Core Processor @ 2.40GHz

All calculations took a total of about 2000 GPU hours. The values of parameters ( $\epsilon$ , number of iterations, etc.) for the attacks are listed in the supplementary materials (Antsiferova et al. 2023).

**Evaluation Metrics** Before calculating metrics’ robustness scores, metric values are transformed with min-max scaling so that the values before the attack lie in the range  $[0,1]$ . To compensate for the nonlinear dependence between metrics (Zhang et al. 2022), we converted all metrics to the same domain before comparison. MDTVSA (Li, Jiang, and Jiang 2021) was used as the primary domain, as it shows the best correlations with MOS among tested metrics according to the MSU Video Quality Metrics benchmark results. We employed the 1-Dimensional Neural Optimal Transport (Korotin, Selikhanovych, and Burnaev 2023) method to build the nonlinear transformation between the distributions of all metrics to one general shape. We also present the results without the nonlinear transformation in the supplementary materials (Antsiferova et al. 2023).

**Absolute and Relative gain.** Absolute gain is calculated as the average difference between the metric values before and after the attack. Relative gain is the average ratio of the difference between the metric values before and after the attack to the metric value before the attack plus 1 (1 is added to avoid division problems, as values before the attack are scaled to  $[0,1]$ ).

$$\begin{aligned} Abs.gain &= \frac{1}{n} \sum_{i=1}^n (f(x'_i) - f(x_i)), \\ Rel.gain &= \frac{1}{n} \sum_{i=1}^n \frac{f(x'_i) - f(x_i)}{f(x_i) + 1}, \end{aligned} \quad (1)$$

where  $n$  is the number of images,  $x_i$  is the clear image,  $x'_i$  — it’s attacked counterpart, and  $f(\cdot)$  is the IQA metric function.

**Robustness score** (Zhang et al. 2022)  $R_{score}$  is defined as the average ratio of maximum allowable change in quality prediction to actual change over all attacked images in a logarithmic scale:

$$R_{score} = \frac{1}{n} \sum_{i=1}^n \log_{10} \left( \frac{\max\{\beta_1 - f(x'_i), f(x_i) - \beta_2\}}{|f(x'_i) - f(x_i)|} \right). \quad (2)$$

As metric values are scaled, we use  $\beta_1 = 1$  and  $\beta_2 = 0$ .

**Wasserstein score** (Kantorovich 1960)  $W_{score}$  and **Energy Distance score** (?)  $E_{score}$  are used to evaluate the statistical differences between distributions of metric values

Training datasets (for UAP attacks)	Type	Number of samples	Resolution	Testing datasets	Type	Number of samples	Resolution
COCO (2014)	Images	300,000	640 × 480	NIPS (2017)	Images	1,000	299 × 299
Pascal VOC (2012)	Image	11,530	500 × 333	Derf’s collection (2001)	Video	24 (~ 10k frames)	1920 × 1080
Vimeo-90k Train set (2019)	Triples of images	2,001	448 × 256	Vimeo 90k Test set (2019)	Triples of images	11,346	448 × 256

Table 2: Summary of the datasets used in our study.

before and after the attack. Large positive values of these scores correspond to a significant upward shift of the metric’s predictions, values near zero indicate the absence of the metric’s response to the attack, and negative ones show a decrease in the metric predictions and the inefficiency of the attack. These scores are defined as corresponding distances between distributions multiplied by the sign of the difference between the mean values before and after the attack:

$$W_{score} = W_1(\hat{P}, \hat{Q}) \cdot \text{sign}(\bar{x}_{\hat{Q}} - \bar{x}_{\hat{P}}),$$

$$W_1(\hat{P}, \hat{Q}) = \inf_{\gamma \in \Gamma(\hat{P}, \hat{Q})} \int_{\mathbb{R}^2} |x - y| d\gamma(x, y) = \int_{-\infty}^{\infty} |\hat{F}_{\hat{P}}(x) - \hat{F}_{\hat{Q}}(x)| dx; \quad (3)$$

$$E_{score} = E(\hat{P}, \hat{Q}) \cdot \text{sign}(\bar{x}_{\hat{Q}} - \bar{x}_{\hat{P}}),$$

$$E(\hat{P}, \hat{Q}) = (2 \cdot \int_{-\infty}^{\infty} (\hat{F}_{\hat{P}}(x) - \hat{F}_{\hat{Q}}(x))^2 dx)^{\frac{1}{2}}, \quad (4)$$

where  $\hat{P}$  and  $\hat{Q}$  are empirical distributions of metric values before and after the attack,  $\hat{F}_{\hat{P}}(x)$  and  $\hat{F}_{\hat{Q}}(x)$  are their respective empirical Cumulative Distribution Functions, and  $\bar{x}_{\hat{P}}$  and  $\bar{x}_{\hat{Q}}$  are their respective sample means.

## Results

The main results of our study are aggregated across the different attack types, training and testing datasets. Tables and figures for other robustness measures, by specific datasets and attacks, are presented in the supplementary materials (Antsiferova et al. 2023) and on the benchmark webpage.

**Metrics that are robust to UAP-based attacks.** Despite the three types of implemented UAP-based attacks resulting in different attack efficiency, the most and least robust metrics for these attacks are similar. MANIQA showed the best robustness score for all amplitudes of Optimized UAP and is within top-3 metrics robust to Generative UAP. This metric uses ViT and applies attention mechanisms across the channel and spatial dimensions, increasing interaction among different regions of images globally and locally. HYPER-IQA showed high resistance to all UAP attacks. Besides FPR, the PAQ-2-PIQ showed the worst energy distance score. The robustness scores of analyzed attacks are provided in Table 3 and illustrated in Fig. 1. Annotations include only five best and five worst methods judged by robustness score for better visibility.

**Metrics that are robust to iterative attacks.** CLIP-IQA shows the best robustness to most iterative attacks, followed by RANK-IQA and MDTVSA. RANK-IQA also offers the

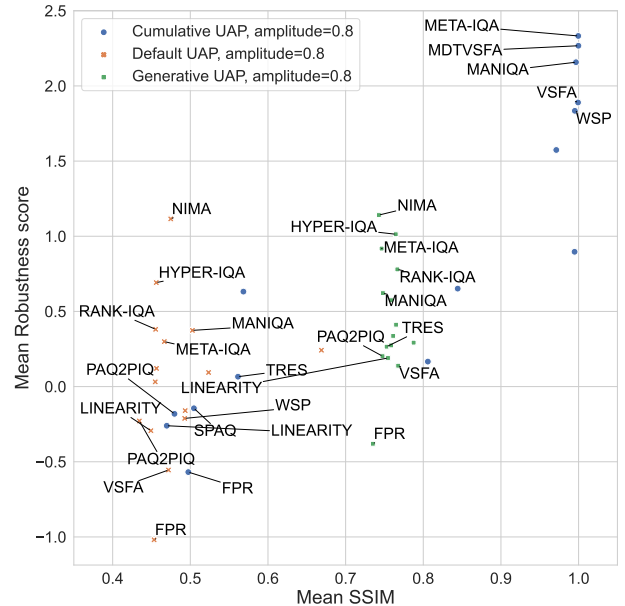


Figure 1: Metrics’ robustness score for UAP-based adversarial attacks and SSIM measured between original and attacked images. The results are averaged for all test datasets.

best resistance to perceptually oriented MADC and Korhonen attacks. These attacks use approaches to reduce the visibility of distortions caused by an attack, which makes it more difficult for them to succeed. The robustness score of analyzed attacks is shown in Table 3 and illustrated in Fig. 2. Annotations include only five best and five worst methods judged by robustness score for better visibility.

**Metrics’ robustness at different levels of perceptual quality loss.** As described in the Benchmark section, we used SSIM, PSNR and MSE as simple proxies for estimating perceptual quality loss of attacks in this study. Fig. 3 shows an averaged robustness score depending on SSIM loss of attacked images for all attacks. It shows that all metrics become less robust to attacks when more quality degradation is allowed. HYPER-IQA’s robustness is more independent from SSIM loss among all metrics. Otherwise, PAQ-2-PIQ, VSFA and FPR are becoming more vulnerable than other metrics with increasing SSIM degradation. Results for other proxy metrics (MSE and PSNR) are provided in the supplementary materials (Antsiferova et al. 2023) and on the

	O-UAP	G-UAP	C-UAP	FGSM	I-FGSM	MI-FGSM	AMI-FGSM	MADC	Korhonen et al.
CLIP-IQA	0.632	0.397	0.067	0.398	<b>0.836</b>	<b>0.821</b>	<b>0.819</b>	0.823	<u>0.812</u>
META-IQA	0.183	<u>-0.029</u>	<u>0.003</u>	0.529	1.307	1.285	1.287	0.934	0.997
RANK-IQA	0.295	0.064	0.180	0.285	<u>1.063</u>	<u>0.891</u>	<u>0.893</u>	<b>0.383</b>	<b>0.763</b>
HYPER-IQA	<u>0.072</u>	<u>-0.094</u>	0.086	<b>-0.406</b>	1.366	1.387	1.396	0.848	1.329
KONCEPT	0.419	0.187	0.435	0.574	1.248	1.066	1.066	0.753	1.042
FPR	1.705	0.846	0.966	0.682	3.344	3.210	3.215	1.703	3.018
NIMA	<u>-0.024</u>	0.046	0.018	0.258	1.203	1.147	1.148	0.959	1.041
WSP	0.784	0.155	0.012	0.405	1.260	1.251	1.257	0.760	0.894
MDTVSFA	0.756	0.359	<u>0.005</u>	<u>0.185</u>	<u>1.011</u>	<u>0.983</u>	<u>0.983</u>	0.914	<u>0.805</u>
LINEARITY	1.022	0.445	0.972	<u>-0.220</u>	1.284	1.218	1.224	0.816	1.204
VSFA	1.151	0.361	0.014	<u>0.306</u>	2.054	2.272	2.274	1.470	1.539
PAQ-2-PIQ	0.943	0.252	0.873	0.578	1.190	1.123	1.125	<u>0.536</u>	0.997
SPAQ	0.605	0.357	0.560	0.266	1.514	1.371	1.375	0.740	1.301
TRES	0.691	0.358	0.634	0.826	1.223	1.209	1.210	0.741	1.173
MANIQA	<b>-0.390</b>	<b>-0.174</b>	<b>-0.003</b>	0.499	1.403	1.225	1.226	<u>0.698</u>	0.843

Table 3: Metrics’ robustness calculated using energy distance score measure to different types of attacks. The results are averaged across test datasets. O-UAP stands for “Optimised-UAP”, G-UAP for “Generative-UAP”, C-UAP for “Cumulative-UAP”.

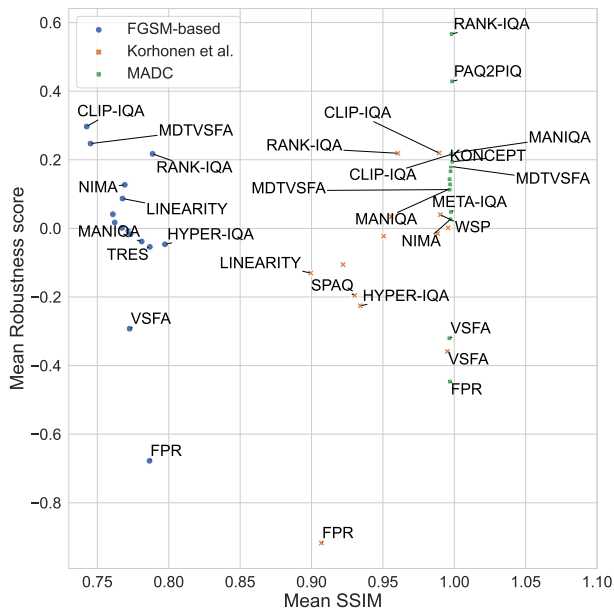


Figure 2: Metrics’ robustness score for iterative adversarial attacks and SSIM measured between original and attacked images. The results are averaged for all test datasets.

benchmark webpage.

**Overall metrics’ robustness comparison.** Table 4 and Fig. 4 show the general results of our study. First, we see that iterative attacks are more efficient against all metrics. However, metrics’ robustness is different for UAP and iterative attacks. We summarised the robustness of all attack types in the table and compared them using various measures. According to absolute and relative gain, the leaders are the same: MANIQA, NIMA and RANK-IQA, and they also perform well based on other measures. META-IQA and

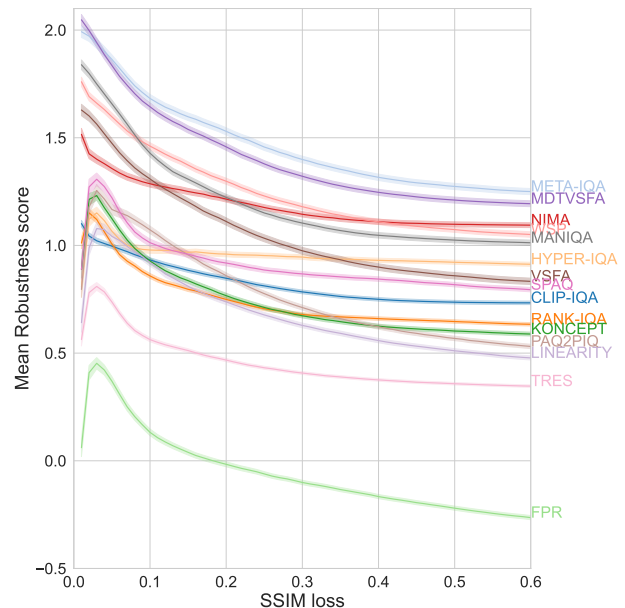


Figure 3: Dependency of metrics’ robustness score of SSIM loss for attacked images (all types of attacks).

MDTVSFA have high robustness scores. Energy measures also show similar results. FPR is the least stable to adversarial attacks, considering all tests and measures.

**One-sided Wilcoxon signed-rank tests.** To study the statistical difference in the results, we conducted one-sided Wilcoxon tests on the values of absolute gains for all pairs of metrics. A table with detailed test results for different types of attacks can be found in the supplementary materials (Antsiferova et al. 2023). All metrics are statistically superior to the FPR metric, which means that FPR can be significantly increased under the influence of any of the con-



	<i>Abs.gain</i> ↓	<i>Rel.gain</i> ↓	<i>R<sub>score</sub></i> ↑	<i>E<sub>score</sub></i> ↓	<i>W<sub>score</sub></i> ↓
CLIP-IQA	0.256 (0.254, 0.258)	0.184 (0.182, 0.185)	0.702 (0.698, 0.707)	0.424	0.256
META-IQA	0.241 (0.238, 0.243)	0.182 (0.180, 0.184)	<b>1.168</b> (1.161, 1.176)	0.324	0.241
RANK-IQA	<u>0.184</u> (0.183, 0.186)	<u>0.12</u> (0.119, 0.122)	0.843 (0.839, 0.848)	0.285	<u>0.184</u>
HYPER-IQA	0.232 (0.228, 0.235)	0.151 (0.149, 0.153)	0.740 (0.735, 0.745)	<u>0.277</u>	0.237
KONCEPT	0.328 (0.326, 0.330)	0.227 (0.225, 0.228)	0.584 (0.579, 0.589)	0.489	0.328
FPR	2.591 (2.568, 2.615)	1.730 (1.714, 1.746)	-0.229(-0.234, -0.224)	1.409	2.591
NIMA	<u>0.17</u> (0.168, 0.172)	<u>0.115</u> (0.114, 0.117)	<u>1.152</u> (1.146, 1.158)	<u>0.239</u>	<b>0.170</b>
WSP	0.380 (0.377, 0.384)	0.276 (0.273, 0.278)	0.893 (0.886, 0.901)	0.449	0.380
MDTVSFA	0.279 (0.277, 0.281)	0.186 (0.184, 0.187)	<u>0.99</u> (0.983, 0.998)	0.447	0.279
LINEARITY	0.683 (0.679, 0.687)	0.447 (0.444, 0.450)	0.267 (0.263, 0.272)	0.780	0.683
VSFA	0.899 (0.891, 0.907)	0.611 (0.606, 0.617)	0.659 (0.650, 0.667)	0.739	0.899
PAQ-2-PIQ	0.521 (0.518, 0.524)	0.341 (0.338, 0.343)	0.449 (0.443, 0.454)	0.675	0.521
SPAQ	0.671 (0.665, 0.678)	0.536 (0.531, 0.542)	0.493 (0.488, 0.499)	0.637	0.671
TRES	0.433 (0.431, 0.435)	0.305 (0.304, 0.307)	0.320 (0.317, 0.323)	0.627	0.433
MANIQA	<b>0.104</b> (0.101, 0.107)	<b>0.078</b> (0.076, 0.08)	0.986 (0.979, 0.993)	<b>0.207</b>	<u>0.175</u>

Table 4: Metrics’ robustness to tested adversarial attacks according to different stability measures. The results for abs. gain, rel. gain and R-score were averaged across different types of attacks and test datasets, so they are presented with confidence intervals. The  $E_{score}$  and  $W_{score}$  were calculated using the whole set of attacked results without averaging.

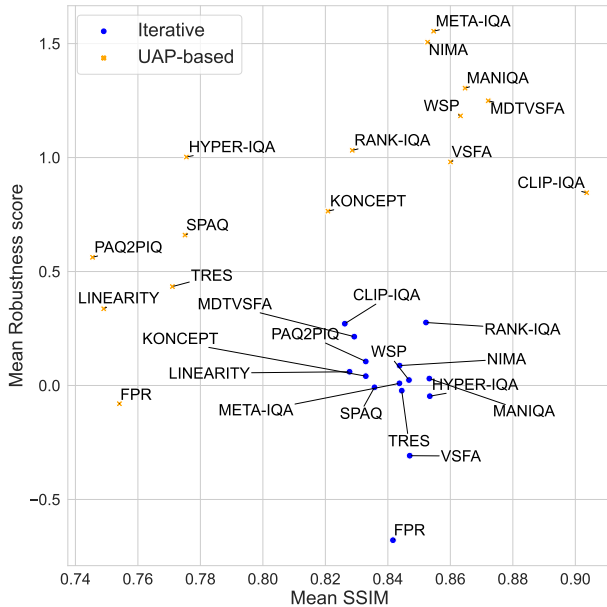


Figure 4: Mean robustness score of compared metrics versus SSIM averages for UAP-based and iterative attacks.

sidered attacks. MANIQA, on the contrary, turns out to be one of the most stable metrics for all attacks on average, but it is inferior to CLIP-IQA on FGSM-based attacks. Overall, the results of the Wilcoxon one-sided tests are consistent with our evaluations of the obtained results.

**Stable metrics feature analysis.** To analyze the relationship of metrics’ architectures with robustness, we summarised the main features of tested metrics in Table 1 of the supplementary materials. A common feature of robust metrics is the usage of the input image cropping or resiz-

ing. High stability to attacks was also shown by META-IQA, which does not transform input images but uses a relatively small backbone network that leverages prior knowledge of various image distortions obtained during so-called meta-learning.

## Conclusion

This paper analyzed the robustness of 15 no-reference image/video-quality metrics to different adversarial attacks. Our analysis showed that all metrics are susceptible to adversarial attacks, but some are more robust than others. MANIQA, META-IQA, NIMA, RANK-IQA and MDTVSFA showed high resistance to adversarial attacks, making their usage in practical applications safer than other metrics. We published this comparison online and are accepting new metrics submissions. This benchmark can be helpful for researchers and companies who want to make their metrics more robust to potential attacks.

In this paper, we revealed ways of cheating on image quality measures, which can be considered to have a potential negative social impact. However, as was discussed in the Introduction, the vulnerabilities of image- and video-quality metrics are already being exploited in some real-life applications. At the same time, only a few studies have been published. We open our findings to the research community to increase the trustworthiness of image/video processing and compression benchmarks. Limitations of our study are listed in the supplementary materials (Antsiferova et al. 2023).

## Acknowledgments

The authors would like to thank the video group of MSU Graphics and Media Laboratory, especially Kirill Malyshev and Vyacheslav Napadovsky, for setting up the infrastructure and helping to receive computational results for this research. The work was supported by a grant for research

centers in the field of artificial intelligence, provided by the Analytical Center in accordance with the subsidy agreement (agreement identifier 000000D730321P5Q0002) and the agreement with the Ivannikov Institute for System Programming dated November 2, 2021 No. 70-2021-00142.

## References

2001. Xiph.org Video Test Media [derf's collection]. <https://media.xiph.org/video/derf/>.
2017. NIPS 2017: Adversarial Learning Development Set. <https://www.kaggle.com/datasets/google-brain/nips-2017-adversarial-learning-development-set>.
- Antsiferova, A.; Abud, K.; Gushchin, A.; Lavrushkin, S.; Shumitskaya, E.; Velikanov, M.; and Vatolin, D. 2023. Comparing the robustness of modern no-reference image- and video-quality metrics to adversarial attacks. *arXiv:2310.06958*.
- Antsiferova, A.; Lavrushkin, S.; Smirnov, M.; Gushchin, A.; Vatolin, D.; and Kulikov, D. 2022. Video compression dataset and benchmark of learning-based video-quality metrics. In *Advances in Neural Information Processing Systems*, volume 35, 13814–13825.
- Bing, M. 2013. A Behind the Scenes Look at How Bing is Improving Image Search Quality. <https://blogs.bing.com/search-quality-insights/2013/08/23/a-behind-the-scenes-look-at-how-bing-is-improving-image-search-quality>.
- Brill, M. H.; Lubin, J.; Costa, P.; Wolf, S.; and Pearson, J. 2004. Accuracy and cross-calibration of video quality metrics: new methods from ATIS/T1A1. *Signal Processing: Image Communication*, 19(2): 101–107.
- Chen, B.; Zhu, L.; Kong, C.; Zhu, H.; Wang, S.; and Li, Z. 2022. No-Reference Image Quality Assessment by Hallucinating Pristine Features. *IEEE Transactions on Image Processing*, 31: 6139–6151.
- Ciaramello, F. M.; and Reibman, A. R. 2011a. Supplemental subjective testing to evaluate the performance of image and video quality estimators. In *Human Vision and Electronic Imaging XVI*, volume 7865, 249–257. SPIE.
- Ciaramello, F. M.; and Reibman, A. R. 2011b. Systematic stress testing of image quality estimators. In *2011 18th IEEE International Conference on Image Processing*, 3101–3104. IEEE.
- Comparison, M. V. C. 2021. MSU Video Codecs Comparison 2021 Part 2: Subjective. [http://www.compression.ru/video/codec\\_comparison/2021/subjective\\_report.html](http://www.compression.ru/video/codec_comparison/2021/subjective_report.html).
- Deng, S.; Han, J.; and Xu, Y. 2020. Vmaf based rate-distortion optimization for video coding. In *2020 IEEE 22nd International Workshop on Multimedia Signal Processing (MMSP)*, 1–6. IEEE.
- Ding, K.; Ma, K.; Wang, S.; and Simoncelli, E. P. 2021. Comparison of full-reference image quality models for optimization of image processing systems. *International Journal of Computer Vision*, 129: 1258–1281.
- Dong, Y.; Liao, F.; Pang, T.; Su, H.; Zhu, J.; Hu, X.; and Li, J. 2018. Boosting adversarial attacks with momentum. In *Proceedings of the IEEE conference on computer vision and pattern recognition*, 9185–9193.
- Everingham, M.; Van Gool, L.; Williams, C. K. I.; Winn, J.; and Zisserman, A. 2012. The PASCAL Visual Object Classes Challenge 2012 (VOC2012) Results. <http://www.pascal-network.org/challenges/VOC/voc2012/workshop/index.html>.
- Fang, Y.; Zhu, H.; Zeng, Y.; Ma, K.; and Wang, Z. 2020. Perceptual quality assessment of smartphone photography. In *Proceedings of the IEEE/CVF Conference on Computer Vision and Pattern Recognition*, 3677–3686.
- Ghildyal, A.; and Liu, F. 2023. Attacking Perceptual Similarity Metrics. *arXiv preprint arXiv:2305.08840*.
- Golestaneh, S. A.; Dadsetan, S.; and Kitani, K. M. 2022. No-reference image quality assessment via transformers, relative ranking, and self-consistency. In *Proceedings of the IEEE/CVF Winter Conference on Applications of Computer Vision*, 1220–1230.
- Goodfellow, I. J.; Shlens, J.; and Szegedy, C. 2015. Explaining and Harnessing Adversarial Examples. In Bengio, Y.; and LeCun, Y., eds., *3rd International Conference on Learning Representations, ICLR 2015, San Diego, CA, USA, May 7-9, 2015, Conference Track Proceedings*.
- Gu, J.; Cai, H.; Dong, C.; Ren, J. S.; Timofte, R.; Gong, Y.; Lao, S.; Shi, S.; Wang, J.; Yang, S.; et al. 2022. NTIRE 2022 challenge on perceptual image quality assessment. In *Proceedings of the IEEE/CVF conference on computer vision and pattern recognition*, 951–967.
- Hosu, V.; Lin, H.; Sziranyi, T.; and Saupe, D. 2020. KonIQ-10k: An ecologically valid database for deep learning of blind image quality assessment. *IEEE Transactions on Image Processing*, 29: 4041–4056.
- Kantorovich, L. V. 1960. Mathematical Methods of Organizing and Planning Production. *Management Science*, 6(4): 366–422.
- Kettunen, M.; Härkönen, E.; and Lehtinen, J. 2019. E-lpips: robust perceptual image similarity via random transformation ensembles. *arXiv preprint arXiv:1906.03973*.
- Klebanov, L. 2005. *N-Distances and their Applications*.
- Korhonen, J.; and You, J. 2022. Adversarial Attacks Against Blind Image Quality Assessment Models. In *Proceedings of the 2nd Workshop on Quality of Experience in Visual Multimedia Applications*, 3–11.
- Korotin, A.; Selikhanovych, D.; and Burnaev, E. 2023. Neural Optimal Transport. In *International Conference on Learning Representations*.
- Kurakin, A.; Goodfellow, I. J.; and Bengio, S. 2018. Adversarial examples in the physical world. In *Artificial intelligence safety and security*, 99–112. Chapman and Hall/CRC.
- Li, D.; Jiang, T.; and Jiang, M. 2019. Quality assessment of in-the-wild videos. In *Proceedings of the 27th ACM International Conference on Multimedia*, 2351–2359.
- Li, D.; Jiang, T.; and Jiang, M. 2020. Norm-in-norm loss with faster convergence and better performance for image quality assessment. In *Proceedings of the 28th ACM International Conference on Multimedia*, 789–797.



- Li, D.; Jiang, T.; and Jiang, M. 2021. Unified quality assessment of in-the-wild videos with mixed datasets training. *International Journal of Computer Vision*, 129: 1238–1257.
- Lin, T.-Y.; Maire, M.; Belongie, S.; Hays, J.; Perona, P.; Ramanan, D.; Dollár, P.; and Zitnick, C. L. 2014. Microsoft coco: Common objects in context. In *Computer Vision–ECCV 2014: 13th European Conference, Zurich, Switzerland, September 6–12, 2014, Proceedings, Part V 13*, 740–755. Springer.
- Liu, H.; and Reibman, A. R. 2016. Software to stress test image quality estimators. In *2016 Eighth International Conference on Quality of Multimedia Experience (QoMEX)*, 1–6. IEEE.
- Liu, X.; Van De Weijer, J.; and Bagdanov, A. D. 2017. Rankiq: Learning from rankings for no-reference image quality assessment. In *Proceedings of the IEEE international conference on computer vision*, 1040–1049.
- Madry, A.; Makelov, A.; Schmidt, L.; Tsipras, D.; and Vladu, A. 2017. Towards deep learning models resistant to adversarial attacks. *arXiv preprint arXiv:1706.06083*.
- MediaEval. 2020. Pixel Privacy: Quality Camouflage for Social Images. <https://multimediaeval.github.io/editions/2020/tasks/pixelprivacy/>.
- Mittal, A.; Soundararajan, R.; and Bovik, A. C. 2012. Making a “completely blind” image quality analyzer. *IEEE Signal processing letters*, 20(3): 209–212.
- Sang, Q.; Zhang, H.; Liu, L.; Wu, X.; and Bovik, A. 2022. On the Generation of Adversarial Samples for Image Quality Assessment. Available at SSRN 4112969.
- Shumitskaya, E.; Antsiferova, A.; and Vatolin, D. S. 2022. Universal Perturbation Attack on Differentiable No-Reference Image- and Video-Quality Metrics. In *33rd British Machine Vision Conference 2022, BMVC 2022, London, UK, November 21–24, 2022*. BMVA Press.
- Shumitskaya, E.; Antsiferova, A.; and Vatolin, D. S. 2023. Fast Adversarial CNN-based Perturbation Attack of No-Reference Image Quality Metrics.
- Siniukov, M.; Antsiferova, A.; Kulikov, D.; and Vatolin, D. 2021. Hacking VMAF and VMAF NEG: vulnerability to different preprocessing methods. In *2021 4th Artificial Intelligence and Cloud Computing Conference*, 89–96.
- Su, J.; Vargas, D. V.; and Sakurai, K. 2019. One pixel attack for fooling deep neural networks. *IEEE Transactions on Evolutionary Computation*, 23(5): 828–841.
- Su, S.; Yan, Q.; Zhu, Y.; Zhang, C.; Ge, X.; Sun, J.; and Zhang, Y. 2020. Blindly assess image quality in the wild guided by a self-adaptive hyper network. In *Proceedings of the IEEE/CVF Conference on Computer Vision and Pattern Recognition*, 3667–3676.
- Su, Y.; and Korhonen, J. 2020. Blind natural image quality prediction using convolutional neural networks and weighted spatial pooling. In *2020 IEEE International Conference on Image Processing (ICIP)*, 191–195. IEEE.
- Talebi, H.; and Milanfar, P. 2018. NIMA: Neural image assessment. *IEEE transactions on image processing*, 27(8): 3998–4011.
- Tu, Z.; Chen, C.-J.; Wang, Y.; Birkbeck, N.; Adsumilli, B.; and Bovik, A. C. 2021. Video Quality Assessment of User Generated Content: A Benchmark Study and a New Model. In *2021 IEEE International Conference on Image Processing (ICIP)*, 1409–1413. IEEE.
- V-Nova. 2023. FFmpeg with LCEVC. <https://docs.v-nova.com/>.
- Wang, J.; Chan, K. C.; and Loy, C. C. 2023. Exploring CLIP for Assessing the Look and Feel of Images. In *AAAI*.
- Wang, Z.; Bovik, A.; Sheikh, H.; and Simoncelli, E. 2004. Image Quality Assessment: From Error Visibility to Structural Similarity. *Image Processing, IEEE Transactions on*, 13: 600 – 612.
- Wang, Z.; and Simoncelli, E. P. 2008. Maximum differentiation (MAD) competition: A methodology for comparing computational models of perceptual quantities. *Journal of Vision*, 8(12): 8–8.
- Xue, T.; Chen, B.; Wu, J.; Wei, D.; and Freeman, W. T. 2019. Video Enhancement with Task-Oriented Flow. *International Journal of Computer Vision (IJCV)*, 127(8): 1106–1125.
- Yang, S.; Wu, T.; Shi, S.; Lao, S.; Gong, Y.; Cao, M.; Wang, J.; and Yang, Y. 2022. Maniqa: Multi-dimension attention network for no-reference image quality assessment. In *Proceedings of the IEEE/CVF Conference on Computer Vision and Pattern Recognition*, 1191–1200.
- Ying, Z.; Niu, H.; Gupta, P.; Mahajan, D.; Ghadiyaram, D.; and Bovik, A. 2020. From patches to pictures (PaQ-2-PiQ): Mapping the perceptual space of picture quality. In *Proceedings of the IEEE/CVF Conference on Computer Vision and Pattern Recognition*, 3575–3585.
- Zhang, K.; Li, D.; Luo, W.; Ren, W.; Stenger, B.; Liu, W.; Li, H.; and Yang, M.-H. 2021. Benchmarking ultra-high-definition image super-resolution. In *Proceedings of the IEEE/CVF international conference on computer vision*, 14769–14778.
- Zhang, R.; Isola, P.; Efros, A. A.; Shechtman, E.; and Wang, O. 2018. The unreasonable effectiveness of deep features as a perceptual metric. In *Proceedings of the IEEE conference on computer vision and pattern recognition*, 586–595.
- Zhang, W.; Li, D.; Min, X.; Zhai, G.; Guo, G.; Yang, X.; and Ma, K. 2022. Perceptual Attacks of No-Reference Image Quality Models with Human-in-the-Loop. *arXiv preprint arXiv:2210.00933*.
- Zhu, H.; Li, L.; Wu, J.; Dong, W.; and Shi, G. 2020. MetalQA: Deep meta-learning for no-reference image quality assessment. In *Proceedings of the IEEE/CVF Conference on Computer Vision and Pattern Recognition*, 14143–14152.
- Zvezdakova, A.; Zvezdakov, S.; Kulikov, D.; and Vatolin, D. 2019. Hacking VMAF with video color and contrast distortion. In *CEUR Workshop Proceedings*, 53–57.

# Supplementary materials: Comparing the robustness of modern no-reference image- and video-quality metrics to adversarial attacks

Anastasia Antsiferova<sup>1,2\*</sup>, Khaled Abud<sup>3\*</sup>, Aleksandr Gushchin<sup>1,2,3\*</sup>, Ekaterina Shumitskaya<sup>3\*</sup>,  
Sergey Lavrushkin<sup>1,2</sup>, Dmitriy Vatolin<sup>1,2,3</sup>

<sup>1</sup>MSU Institute for Artificial Intelligence

<sup>2</sup>ISP RAS Research Center for Trusted Artificial Intelligence

<sup>3</sup>Lomonosov Moscow State University

{aantsiferova, khaled.abud, alexander.gushchin, ekaterina.shumitskaya, sergey.lavrushkin, dmitriy}@graphics.cs.msu.ru

## Limitations

This study provides IQA/VQA metrics robustness analysis to the nine popular adversarial attacks. Metrics that are robust to these attacks may appear vulnerable to other existing attacks and newly developed ones. We did not analyse the perceptual quality of attacked images for several reasons. Firstly, our aim was to investigate the general limitations of metrics usage as loss components or as measures in benchmarks. In real-life scenarios, the developers of video codecs or other processing methods would not use extreme attacks that drop down perceptual quality, but it's probable in benchmarking cases. Secondly, according to our knowledge, the intensity of an attack correlates with perceptual quality, which means that reducing the visibility of our attacks will cause general success but will not change the obtained results significantly.

For now, we have not investigated ways to eliminate applied adversarial attacks. However, there are benchmarks of adversarial defences (Croce et al. 2020; rob) created for computer vision tasks. We are working on the release of our own benchmark of defences against adversarial attacks on quality metrics.

This benchmark can be used as a reference to the general robustness of popular IQA/VQA metrics to popular adversarial attacks. However, the robustness may change when you apply different transformations to an attacked image. For example, compression is a way to defend metrics from adversarial attacks (Guo et al. 2017), which means that this leaderboard may change if we compress attacked images in our pipeline. Other transformations may include image super-resolution, deblurring, deblocking, etc. In this study, we did not investigate attacks together with image-processing defence techniques. First of all, there are too many types of them and we consider starting with compression. Secondly, according to our preliminary results with compression of attacked images, its application reduces attacks' success proportionally to its value. It means that if the metric is highly vulnerable, the compression will unlikely remove the attack completely. The same effect may appear with other processing, but now it remains a promising topic for further research.

\*These authors contributed equally.

## Additional experimental details

### Datasets description

For testing, we have used images and video from five datasets:

- **COCO** (Lin et al. 2014) has become a standard benchmark for evaluating and training computer vision algorithms. It has facilitated the development of state-of-the-art models in tasks like object detection, instance segmentation, image captioning, and visual question answering. Its large-scale, diverse, and accurately annotated data make it a valuable resource for advancing the field of computer vision.
- **Pascal VOC 2012** (Everingham et al. 2012) is a widely used benchmark dataset for object recognition and detection tasks in computer vision. It is part of the PASCAL Visual Object Classes (VOC) Challenge, which was organized annually from 2005 to 2012.
- **Vimeo-90k** (Xue et al. 2019) is a large-scale high-quality video dataset for lower-level video processing. It proposes three different video processing tasks: frame interpolation, video denoising/deblocking, and video super-resolution. We used triplets subset that consists of 3-frame sequences with a fixed resolution of  $448 \times 256$ , extracted from 15K selected video clips from Vimeo-90K. This dataset is designed for temporal frame interpolation.
- **NIPS 2017: Adversarial Learning Development Set** (nip 2017) was organized by Google Brain for Competition on Adversarial Examples and Defenses within the NIPS 2017 competition track. This dataset contains the development images for this competition.
- **Derf's collection (blue sky video)** (der 2001) is a collection of videos with various content.

The datasets are publicly available and can be acquired by the following links:

- COCO with CC-BY 4.0 license. <https://cocodataset.org/#home>
- Pascal VOC 2012. <http://host.robots.ox.ac.uk/pascal/VOC/>
- Vimeo-90k. <http://toflow.csail.mit.edu/>

- NIPS 2017: Adversarial Learning Development Set. <https://www.kaggle.com/datasets/google-brain/nips-2017-adversarial-learning-development-set>
- Derf’s collection (blue\_sky sequence) with no copyright or restrictions on the use. <https://media.xiph.org/video/derf/>

We used PyAV python library (pya 2023) for splitting the videos into individual frames.

```

1 import av
2 container = av.open(path_to_video)
3 video_stream = container.streams.video
  [0]
4 frame_array = container.decode(
  video_stream)

```

### Quality assessment methods description

Table 2 lists image and video quality assessment methods used in our experiments. We provide links to original implementations, but the original code was slightly modified to operate within our framework. Method parameters were not changed. All implementations use the PyTorch library, which allows the computation of the gradient of loss w.r.t. input image uniformly for all metrics. All considered quality assessment methods monotonically increase as image/video quality does.

**Analysis of metrics’ features that make them stable to adversarial attacks** We summarised implementation details of tested metrics to analyse features that could lead to adversarial robustness in 1. Robust META-IQA uses a relatively small backbone network but efficiently leverages prior knowledge of various image distortions obtained during so-called meta-learning. MDTVSFA metric is the only metric that showed good overall stability and has high correlations with human perception (Antsiferova et al. 2022), and its key features include training on multiple IQA datasets at once. Notably, the CLIP-IQA metric, which adapted CLIP architecture for IQA tasks, shows good resistance to FGSM-based attacks, but the average stability across all attacks is not very high. The worst stability is consistently shown by the FPR metric. It may be caused by its extremely unusual architecture for the NR-IQA task, which includes a Siamese network and an attempt to “hallucinate” the features of the pseudo-reference image from a distorted one.

### Adversarial attacks description

Table 3 contains parameters description for employed adversarial attacks. AMI-FGSM (Sang et al. 2022), Korhonen et al. (Korhonen and You 2022) and MADC (Wang and Simoncelli 2008) did not have original code so we implemented them using algorithms 1, 2, 3. Our implementations are available in *link is hidden for a blind review*. We chose  $\epsilon$  equal to  $\frac{10}{255}$  for all attacks if applicable because this value is widely used for attacks on classifiers. For iterative attacks we tried different amounts of iterations in the range of 1–100, however, due to the computation complexity we used 1–10 iterations depending on attack success and speed. For UAP attacks training we tried a number of epochs in the range of 1–10 and dataset size in the range of 1,000–10,000. Optimal attack success on validation was reached when 5 iterations and 6,000 dataset size was used (see Figure 1).

---

### Algorithm 1: AMI-FGSM adversarial attack

---

**Inputs:** image  $I$ , target quality-metric  $M$ , restriction on  $l_p$  norm of the perturbation  $\epsilon$ , number of iterations  $n_{iters}$   
**Output:** adversarial image  $I_{adv}$

```

 $I_{adv} = I$ 
 $\alpha = \frac{\epsilon}{n_{iters}}$ 
 $\nu = 1$ 
 $g_{prev} = 0$ 
for  $i = 1$  to  $n_{iters}$  do
   $score = M(I_{adv})$ 
   $loss = 1 - \frac{score}{M_{range}}$ 
  {Compute the gradient  $g$  with respect to  $I_{adv}$ }
   $g = g + \nu \cdot g_{prev}$ 
   $g = sign(g)$ 
   $I_{adv} = I_{adv} - \alpha \cdot g$ 
end for

```

---



---

### Algorithm 2: Korhonen et al. adversarial attack

---

**Inputs:** image  $I$ , target quality-metric  $M$ , step size  $\alpha$ , number of iterations  $n_{iters}$   
**Output:** adversarial image  $I_{adv}$

```

 $I_{adv} = I$ 
 $sp\_map = SpatialActivityMap(I)$ 
for  $i = 1$  to  $n_{iters}$  do
   $score = M(I_{adv})$ 
   $loss = 1 - \frac{score}{M_{range}}$ 
  {Compute the gradient  $g$  with respect to  $I_{adv}$ }
   $g = g \cdot sp\_map$ 
  {Update  $I_{adv}$  using optimizer step with  $lr = \alpha$ }
end for

```

---

### Evaluation metrics description

We used MinMaxScaler from the preprocessing module of the Scikit-learn library (Pedregosa et al. 2011) to normalize the metric values to the range [0,1]. To calculate Wasserstein- and Energy-distance, the corresponding functions from SciPy’s (Virtanen et al. 2020) stats module were used (`wasserstein_distance(x, y)` and `energy_distance(x, y)`). We employed a small neural network consisting of four linear layers as a model for metrics domain transformation, as shown in a one-dimensional example in the repository (NOT 2023). It was trained according to algorithm 4 described in (Korotin, Selikhanovych, and Burnaev 2023) for metric scores on the NIPS 2017 dataset.

### Evaluation pipeline scheme

Fig. 2 visualises the pipeline of our benchmark.

### Additional experimental results

#### Results on different test datasets

In the paper, we showed the results combined for all test datasets as they did not differ much between each other. Table 5 contains robustness scores for metrics on NIPS 2017,

Metric	$R_{score} \uparrow$	CNN-backbone	Number of params	Train datasets	Input transformations
META-IQA	1.168	ResNet-18	13.2M	AVA: 255,000 images	ImageNet Normalization
NIMA	1.152	MobileNetV2	2.24M		224 × 224 resize
MDTVSFA	0.99	ResNet-50	24.05M	LIVE-VQC, LIVE-Qualcomm, KoNViD-1k, CVD2014	ImageNet Normalization
MANIQA	0.986	ViT-B/8	135.62M	LIVE, CSIQ, TID2013, KADID-10K, PIPAL	224 × 224 crop
WSP	0.893	ResNet-101	46.7M	Subset of KonIq-10K	224 × 224 resize
RANK-IQA	0.843	VGG-16	134.26M		
HYPER-IQA	0.740	ResNet-50	27.38M	LIVE, KonIQ-10K, BID, CSIQ	ImageNet Normalization, 224 × 224 resize
CLIP-IQA	0.702	ResNet-50			
VSFA	0.659	ResNet-50	24.06M	KoNViD-1k: 1,000 videos	ImageNet Normalization
KONCEPT	0.584	InceptionResNetV2	59.82M	KonIQ-10k: 10,000 images	Normalization (0.5, 0.5)
SPAQ	0.493	ResNet-50	23.5M	Proposed (11,000 images)	224 × 224 crop
PAQ2PIQ	0.449	ResNet-18	11M	Proposed (40,000 images)	No
TRES	0.320	ResNet-50	152.5M		
LINEARITY	0.267	ResNeXt-101	90M	KonIQ-10k: 10,000 images	ImageNet Normalization
FPR	-0.229	Custom	16.6M	TID2013, LIVE, CSIQ, KADID-10k	

Table 1: Implementation details of evaluated metrics.

VIMEO and “Blue sky” video from Derf’s collection separately. The results on NIPS 2017 and VIMEO datasets are similar, while leaders in stability scores are different for “Blue sky”. This video sequence differs from other datasets for two reasons. First, the resolution is bigger while UAP attacks were trained on a small resolution. Second, the attacks were applied frame-by-frame and all frames within one video sequence are relatively similar while images from other test datasets vary a lot.

### Results for different stability measurement scores

Tables 7, 9, 11, 13 show metrics robustness to all types of tested adversarial attacks by different stability measurement scores. Results are very similar for absolute and relative gain, as well as for energy distance (shown in the main part of the paper) and Wasserstein score. The leaders differ a bit only according to robustness score (Zhang et al. 2022) which is likely caused by its non-linearity (it applies logarithm).

Fig. 3 shows supplemental visualisations for adversarial attacks efficiency depending on SSIM between original and attacked images. The robustness score is averaged within a sliding window of 0.1 (in the main part of the paper, this chart shows results averaged for all examples with SSIM loss that is less or equal to each point on the x-axis). Fig. 4 shows supplemental results for iterative attacks efficiency depending on PSNR loss.

### Results for resistance to UAP attacks trained on different datasets

Table 14 compares metrics robustness to UAP adversarial attacks trained on different datasets (COCO and Pascal VOC). Leaderboard and general stability results are the same. On the one hand, it proves that trained perturbations are stable. On the other hand, these datasets contain images of similar resolution, when perturbation for bigger resolution may be different. Investigating stability to perturbations of bigger resolution is a subject for further research.

### Results without metrics domain transformation

Table 15 shows the results for different stability score measures without domain transformation of metrics. As we described in the paper, we used optimal transport to transfer all metrics’ scales to one (MDTVSFA). We noticed that if we do not apply domain transformation, the leaderboard of tested metrics does not change for all of the robustness scores. In cases when domain transformation is time- or resources-consuming, we assume that this step can be omitted, at least for comparing metrics from our list. Some new metrics may have unusual distributions of values that require transformation for getting correct comparison results.

### Example usage and reproducibility

Code for reproducing our main results is available in the repository *link is hidden for a blind review*. It runs all types of trained attacks for one metric on all available datasets and evaluates its robustness according to our methodology. The

Table 2: Source code to official implementations of quality assessment methods.

	Metric	Year	Image or Video	Implementation
	CLIP-IQA (Wang, Chan, and Loy 2023)	2022	Image	<a href="https://github.com/IceClear/CLIP-IQA">https://github.com/IceClear/CLIP-IQA</a>
	META-IQA (Zhu et al. 2020)	2020	Image	<a href="https://github.com/zhuhanheng/MetaIQA">https://github.com/zhuhanheng/MetaIQA</a>
	RANK-IQA (Liu, Van De Weijer, and Bagdanov 2017)	2017	Image	<a href="https://github.com/YunanZhu/Pytorch-TestRankIQA">https://github.com/YunanZhu/Pytorch-TestRankIQA</a>
	HYPER-IQA (Su et al. 2020)	2020	Image	<a href="https://github.com/chaofengc/IQA-PyTorch">https://github.com/chaofengc/IQA-PyTorch</a>
	KONCEPT (Hosu et al. 2020)	2020	Image	<a href="https://github.com/ZhengyuZhao/koniq-PyTorch">https://github.com/ZhengyuZhao/koniq-PyTorch</a>
	FPR (Chen et al. 2022)	2022	Image	<a href="https://github.com/Baoliang93/FPR">https://github.com/Baoliang93/FPR</a>
	NIMA (Talebi and Milanfar 2018)	2018	Image	<a href="https://github.com/truskovskiyk/nima.pytorch/tree/v1">https://github.com/truskovskiyk/nima.pytorch/tree/v1</a>
	WSP (Su and Korhonen 2020)	2020	Image	<a href="https://github.com/yichengsu/ICIP2020-WSP-IQA">https://github.com/yichengsu/ICIP2020-WSP-IQA</a>
	MDTVSFA (Li, Jiang, and Jiang 2021)	2021	Video	<a href="https://github.com/lidq92/MDTVSFA">https://github.com/lidq92/MDTVSFA</a>
	LINEARITY (Li, Jiang, and Jiang 2020)	2020	Image	<a href="https://github.com/lidq92/LinearityIQA">https://github.com/lidq92/LinearityIQA</a>
	VSFA (Li, Jiang, and Jiang 2019)	2019	Video	<a href="https://github.com/lidq92/VSFA">https://github.com/lidq92/VSFA</a>
	PAQ2PIQ (Ying et al. 2020)	2020	Image	<a href="https://github.com/baidut/paq2piq">https://github.com/baidut/paq2piq</a>
	SPAQ (Fang et al. 2020)	2020	Image	<a href="https://github.com/h4nwei/SPAQ">https://github.com/h4nwei/SPAQ</a>
	TRES (Golestaneh, Dadsetan, and Kitani 2022)	2022	Image	<a href="https://github.com/isalirezag/TReS">https://github.com/isalirezag/TReS</a>
	MANIQA (Yang et al. 2022)	2022	Image	<a href="https://github.com/IIGROUP/MANIQA">https://github.com/IIGROUP/MANIQA</a>

repository contains several utility files containing primary functions and a demo Jupyter Notebook file which contains an example of launching all the attacks and estimating their results. To reproduce the results, one can simply run all the cells in it sequentially.

We also provide the results of our runs for all the metrics as of this writing. They can be downloaded from *link is hidden for a blind review* as a dataframe in feather format. `Pandas.read_feather()` can be used to open the file with Python and Pandas library. It contains metrics scores before and after each attack and also SSIM, PSNR and MSE measures between original images and their attacked counterparts.

## References

???? <https://ml.cs.tsinghua.edu.cn/adv-bench/#/>.

2001. <https://media.xiph.org/video/derf/>.

2017. <https://www.kaggle.com/datasets/google-brain/nips-2017-adversarial-learning/-development-set>.

2023. <https://pyav.org/docs/stable/#>.

2023. <https://github.com/iamalexkorotin/NeuralOptimalTransport>.

Antsiferova, A.; Lavrushkin, S.; Smirnov, M.; Gushchin, A.; Vatolin, D.; and Kulikov, D. 2022. Video compression dataset and benchmark of learning-based video-quality metrics. In *Advances in Neural Information Processing Systems*, volume 35, 13814–13825.

Chen, B.; Zhu, L.; Kong, C.; Zhu, H.; Wang, S.; and Li, Z. 2022. No-Reference Image Quality Assessment by Hallucinating Pristine Features. *IEEE Transactions on Image Processing*, 31: 6139–6151.

Croce, F.; Andriushchenko, M.; Sehwag, V.; DeBenedetti, E.; Flammarion, N.; Chiang, M.; Mittal, P.; and Hein, M. 2020. RobustBench: a standardized adversarial robustness benchmark. *arXiv preprint arXiv:2010.09670*.

Everingham, M.; Van Gool, L.; Williams, C. K. I.; Winn, J.; and Zisserman, A. 2012. The PASCAL Visual Object Classes Challenge 2012 (VOC2012) Results. <http://www.pascal-network.org/challenges/VOC/voc2012/workshop/index.html>.

Fang, Y.; Zhu, H.; Zeng, Y.; Ma, K.; and Wang, Z. 2020. Perceptual quality assessment of smartphone photography. In *Proceedings of the IEEE/CVF Conference on Computer Vision and Pattern Recognition*, 3677–3686.

Golestaneh, S. A.; Dadsetan, S.; and Kitani, K. M. 2022.

Table 3: Attacks description, where  $\epsilon$  is the restriction on  $l_\infty$ -norm of adversarial perturbation and  $\alpha$  is the step size.

Attack method	$\epsilon$	$\alpha$	$n_{iters}$	$n_{epochs}$	Original Implementation
FGSM	$\frac{10}{255}$	$\frac{\epsilon}{n_{iters}}$	1	-	<a href="https://github.com/1Konny/FGSM">https://github.com/1Konny/FGSM</a>
I-FGSM	$\frac{10}{255}$	$\frac{\epsilon}{n_{iters}}$	10	-	<a href="https://github.com/1Konny/FGSM">https://github.com/1Konny/FGSM</a>
MIFGSM	$\frac{10}{255}$	$\frac{\epsilon}{n_{iters}}$	10	-	<a href="https://github.com/Harry24k/adversarial-attacks-pytorch">https://github.com/Harry24k/adversarial-attacks-pytorch</a>
AMI-FGSM	$\frac{10}{255}$	$\frac{\epsilon}{n_{iters}}$	10	-	Implementation described in algorithm 1 Description from paper (Sang et al. 2022)
Optimised-UAP	$\frac{25}{255}$	-	-	5	<a href="https://github.com/katiashh/UAP_Attack_on_Quality_Metrics">https://github.com/katiashh/UAP_Attack_on_Quality_Metrics</a>
Cumulative-UAP	$\frac{25}{255}$	-	-	5	<a href="https://github.com/BXuan694/Universal-Adversarial-Perturbation">https://github.com/BXuan694/Universal-Adversarial-Perturbation</a>
Generative-UAP	$\frac{10}{255}$	-	-	1	Adaptation of code from <a href="https://github.com/OmidPoursaeed/Generative-Adversarial-Perturbations">https://github.com/OmidPoursaeed/Generative-Adversarial-Perturbations</a>
Korhonen et al.	-	0.005	10	-	Implementation described in algorithm 2 Description from paper (Korhonen and You 2022)
MADC	$\frac{10}{255}$	0.001	8	-	Implementation described in algorithm 3 Description from paper (Wang and Simoncelli 2008)

---

Algorithm 3: MADC adversarial attack

---

**Inputs:** image  $I$ , target quality-metric  $M$ , restriction on  $l_p$  norm of the perturbation  $\epsilon$ , step size  $\alpha$  number of iterations  $n_{iters}$   
**Output:** adversarial image  $I_{adv}$   
 $I_{adv} = I$   
**for**  $i = 1$  to  $n_{iters}$  **do**  
     $score = M(I_{adv})$   
     $loss = 1 - \frac{score}{M.range}$   
    {Compute the gradient  $g1$  with respect to  $I_{adv}$ }  
     $loss = \sqrt{mean((I_{adv} - I)^2)}$   
    {Compute the gradient  $g2$  with respect to  $I_{adv}$ }  
     $pg = g1 - \frac{g2^T \cdot g1}{g2^T \cdot g2} \cdot g2$   
     $pg = sign(pg)$   
     $I_{adv} = I_{adv} - \alpha \cdot pg$   
     $cur\_norm = \sqrt{mean((I_{adv} - I)^2)}$   
    **while**  $cur\_norm > \epsilon$  **do**  
        {Compute the gradient  $g2$  with respect to  $I_{adv}$ }  
         $g2 = sign(g2)$   
         $I_{adv} = I_{adv} - 0.0005 \cdot g2$   
         $cur\_norm = \sqrt{mean((I_{adv} - I)^2)}$   
    **end while**  
**end for**

---

No-reference image quality assessment via transformers, relative ranking, and self-consistency. In *Proceedings of the IEEE/CVF Winter Conference on Applications of Computer Vision*, 1220–1230.

Guo, C.; Rana, M.; Cisse, M.; and Maaten, L. 2017. Countering Adversarial Images using Input Transformations.

Hosu, V.; Lin, H.; Sziranyi, T.; and Saupe, D. 2020. KonIQ-10k: An ecologically valid database for deep learning of

blind image quality assessment. *IEEE Transactions on Image Processing*, 29: 4041–4056.

Korhonen, J.; and You, J. 2022. Adversarial Attacks Against Blind Image Quality Assessment Models. In *Proceedings of the 2nd Workshop on Quality of Experience in Visual Multimedia Applications*, 3–11.

Korotin, A.; Selikhanovych, D.; and Burnaev, E. 2023. Neural Optimal Transport. In *International Conference on Learning Representations*.

Li, D.; Jiang, T.; and Jiang, M. 2019. Quality assessment of in-the-wild videos. In *Proceedings of the 27th ACM International Conference on Multimedia*, 2351–2359.

Li, D.; Jiang, T.; and Jiang, M. 2020. Norm-in-norm loss with faster convergence and better performance for image quality assessment. In *Proceedings of the 28th ACM International Conference on Multimedia*, 789–797.

Li, D.; Jiang, T.; and Jiang, M. 2021. Unified quality assessment of in-the-wild videos with mixed datasets training. *International Journal of Computer Vision*, 129: 1238–1257.

Lin, T.-Y.; Maire, M.; Belongie, S.; Hays, J.; Perona, P.; Ramanan, D.; Dollár, P.; and Zitnick, C. L. 2014. Microsoft coco: Common objects in context. In *Computer Vision—ECCV 2014: 13th European Conference, Zurich, Switzerland, September 6–12, 2014, Proceedings, Part V 13*, 740–755. Springer.

Liu, X.; Van De Weijer, J.; and Bagdanov, A. D. 2017. Rankiqa: Learning from rankings for no-reference image quality assessment. In *Proceedings of the IEEE international conference on computer vision*, 1040–1049.

Pedregosa, F.; Varoquaux, G.; Gramfort, A.; Michel, V.; Thirion, B.; Grisel, O.; Blondel, M.; Prettenhofer, P.; Weiss, R.; Dubourg, V.; et al. 2011. Scikit-learn: Machine learning in Python. *Journal of machine learning research*, 12(Oct): 2825–2830.

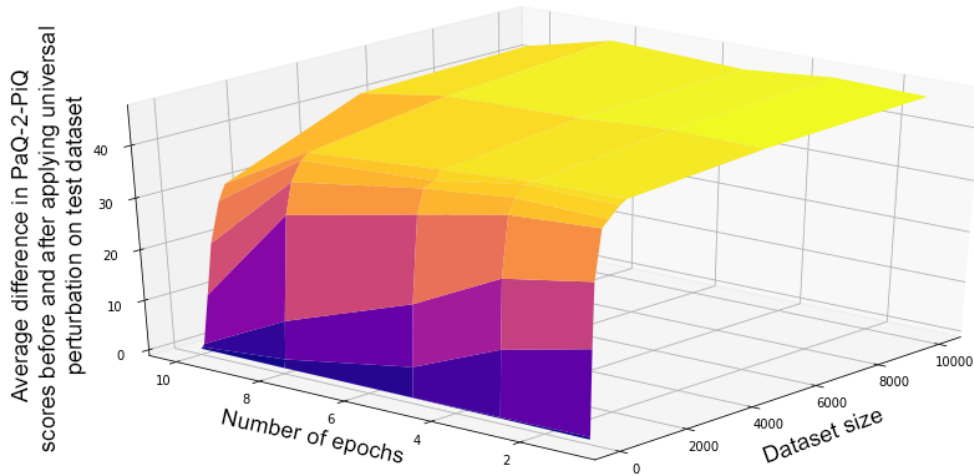


Figure 1: Visualization of experimental search for optimal hyper-parameters (number of epochs and dataset size) for Optimized UAP attack when attacking PaQ-2-PiQ NR quality metric.

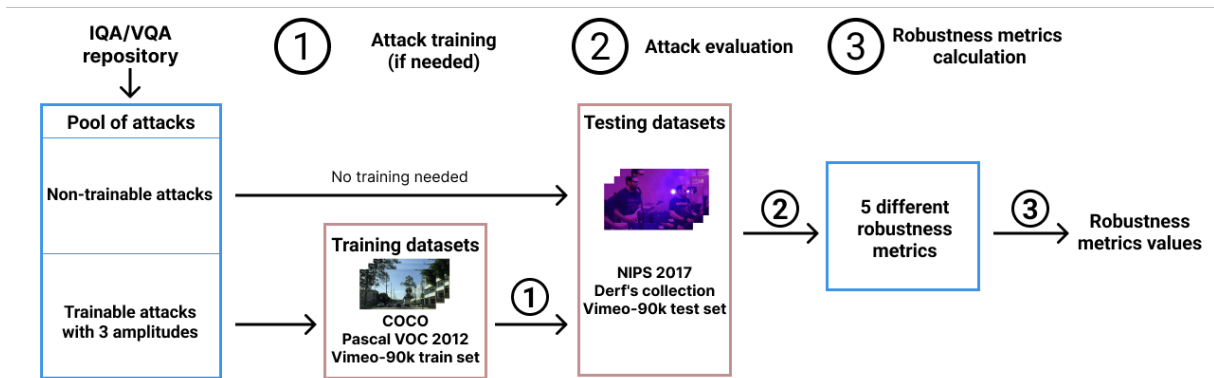


Figure 2: Evaluation pipeline scheme.

Sang, Q.; Zhang, H.; Liu, L.; Wu, X.; and Bovik, A. 2022. On the Generation of Adversarial Samples for Image Quality Assessment. Available at SSRN 4112969.

Su, S.; Yan, Q.; Zhu, Y.; Zhang, C.; Ge, X.; Sun, J.; and Zhang, Y. 2020. Blindly assess image quality in the wild guided by a self-adaptive hyper network. In *Proceedings of the IEEE/CVF Conference on Computer Vision and Pattern Recognition*, 3667–3676.

Su, Y.; and Korhonen, J. 2020. Blind natural image quality prediction using convolutional neural networks and weighted spatial pooling. In *2020 IEEE International Conference on Image Processing (ICIP)*, 191–195. IEEE.

Talebi, H.; and Milanfar, P. 2018. NIMA: Neural image assessment. *IEEE transactions on image processing*, 27(8): 3998–4011.

Virtanen, P.; Gommers, R.; Oliphant, T. E.; Haberland, M.; Reddy, T.; Cournapeau, D.; Burovski, E.; Peterson, P.; Weckesser, W.; Bright, J.; van der Walt, S. J.; Brett, M.;

Wilson, J.; Millman, K. J.; Mayorov, N.; Nelson, A. R. J.; Jones, E.; Kern, R.; Larson, E.; Carey, C. J.; Polat, İ.; Feng, Y.; Moore, E. W.; VanderPlas, J.; Laxalde, D.; Perktold, J.; Cimrman, R.; Henriksen, I.; Quintero, E. A.; Harris, C. R.; Archibald, A. M.; Ribeiro, A. H.; Pedregosa, F.; van Mulbregt, P.; and SciPy 1.0 Contributors. 2020. SciPy 1.0: Fundamental Algorithms for Scientific Computing in Python. *Nature Methods*, 17: 261–272.

Wang, J.; Chan, K. C.; and Loy, C. C. 2023. Exploring CLIP for Assessing the Look and Feel of Images. In *AAAI*.

Wang, Z.; and Simoncelli, E. P. 2008. Maximum differentiation (MAD) competition: A methodology for comparing computational models of perceptual quantities. *Journal of Vision*, 8(12): 8–8.

Xue, T.; Chen, B.; Wu, J.; Wei, D.; and Freeman, W. T. 2019. Video Enhancement with Task-Oriented Flow. *International Journal of Computer Vision (IJCV)*, 127(8): 1106–1125.

Yang, S.; Wu, T.; Shi, S.; Lao, S.; Gong, Y.; Cao, M.; Wang,



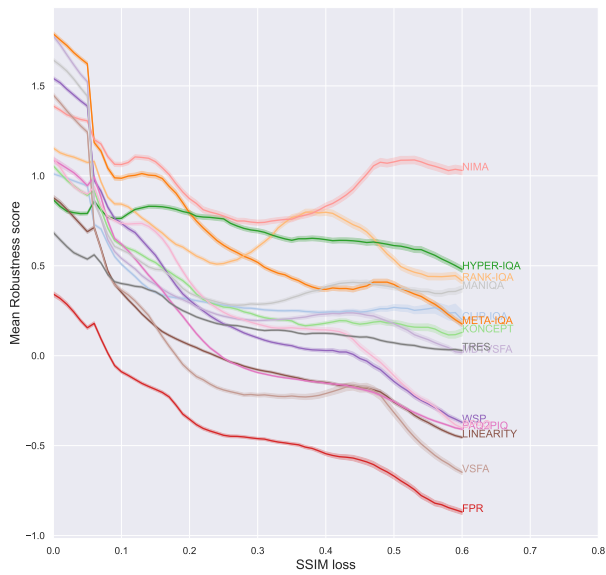


Figure 3: Dependency of metrics robustness scores on SSIM loss averaged in a 0.1 sliding window for attacked images (all types of attacks).

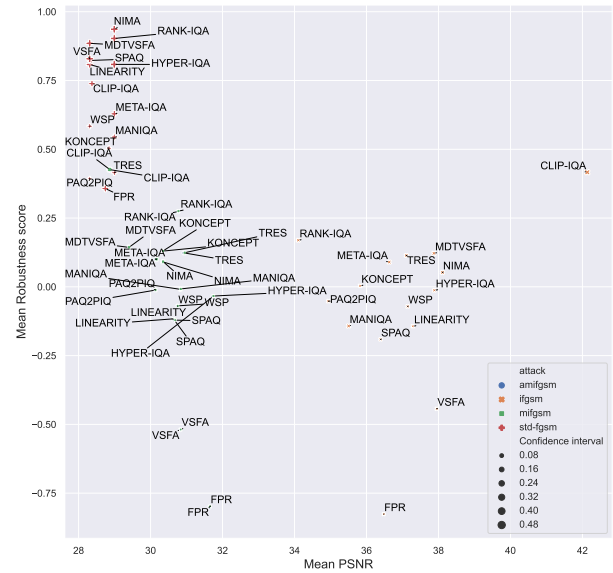


Figure 4: Mean robustness score of compared metrics versus mean PSNR for iterative attacks.

J.; and Yang, Y. 2022. Maniqa: Multi-dimension attention network for no-reference image quality assessment. In *Proceedings of the IEEE/CVF Conference on Computer Vision and Pattern Recognition*, 1191–1200.

Ying, Z.; Niu, H.; Gupta, P.; Mahajan, D.; Ghadiyaram, D.; and Bovik, A. 2020. From patches to pictures (PaQ-2-PiQ): Mapping the perceptual space of picture quality. In *Proceedings of the IEEE/CVF Conference on Computer Vision and Pattern Recognition*, 3575–3585.

Zhang, W.; Li, D.; Min, X.; Zhai, G.; Guo, G.; Yang, X.; and Ma, K. 2022. Perceptual Attacks of No-Reference Image Quality Models with Human-in-the-Loop. *arXiv preprint arXiv:2210.00933*.

Zhu, H.; Li, L.; Wu, J.; Dong, W.; and Shi, G. 2020. MetaIQA: Deep meta-learning for no-reference image quality assessment. In *Proceedings of the IEEE/CVF Conference on Computer Vision and Pattern Recognition*, 14143–14152.

---

**Algorithm 4: Results evaluation algorithm**

---

**Inputs:** metric scores before the attack  $X_{clear}$  and after  $X_{attacked}$  (vectors of length  $N$ ), trained domain transformation model  $T(\cdot)$ . (Training algorithm is described in (Korotin, Selikhanovych, and Burnaev 2023) (Algorithm 1))

**Output:** calculated scores  $Abs.gain$ ,  $Rel.gain$ ,  $R_{score}$ ,  $E_{score}$  and  $W_{score}$ .

```
 $\hat{X}_{clear} = T(X_{clear})$  {Apply N.O.T. domain transformation}
 $\hat{X}_{attacked} = T(X_{attacked})$  {Scale to range [0, 1]}
 $\hat{X}_{clear} = (\hat{X}_{clear} - \min(\hat{X}_{clear})) / (\max(\hat{X}_{clear}) - \min(\hat{X}_{clear}))$ 
 $\hat{X}_{attacked} = (\hat{X}_{attacked} - \min(\hat{X}_{clear})) / (\max(\hat{X}_{clear}) - \min(\hat{X}_{clear}))$ 
{Evaluate}
 $S_{abs} = 0$ 
 $S_{rel} = 0$ 
 $S_R = 0$ 
for  $i = 1$  to  $N$  do
     $S_{abs} += \hat{X}_{i,attacked} - \hat{X}_{i,clear}$ 
     $S_{rel} += (\hat{X}_{i,attacked} - \hat{X}_{i,clear}) / (\hat{X}_{i,clear} + 1)$ 
     $S_R += \log_{10}(\max\{1, \frac{\hat{X}_{i,attacked} - \hat{X}_{i,clear}}{|\hat{X}_{i,attacked} - \hat{X}_{i,clear}|}\})$ 
end for
 $Abs.gain = \frac{1}{N} \sum_{i=1}^N S_{abs}$ 
 $Rel.gain = \frac{1}{N} \sum_{i=1}^N S_{rel}$ 
 $R_{score} = \frac{1}{N} \sum_{i=1}^N S_R$ 

 $W_{score} = \text{sign}(\frac{1}{N} \sum_{i=1}^N \hat{X}_{i,attacked} - \frac{1}{N} \sum_{i=1}^N \hat{X}_{i,clear}) \cdot \text{wasserstein\_distance}(\hat{X}_{clear}, \hat{X}_{attacked})$ 
 $E_{score} = \text{sign}(\frac{1}{N} \sum_{i=1}^N \hat{X}_{i,attacked} - \frac{1}{N} \sum_{i=1}^N \hat{X}_{i,clear}) \cdot \text{energy\_distance}(\hat{X}_{clear}, \hat{X}_{attacked})$ 
return  $Abs.gain$ ,  $Rel.gain$ ,  $R_{score}$ ,  $W_{score}$ ,  $E_{score}$ 
```

---

NIPS 2017 dataset, with domain transform, Energy score									
Attack Amplitude	Optimized-UAP			Generative-UAP			Cumulative-UAP		
	0.2	0.4	0.8	0.2	0.4	0.8	0.2	0.4	0.8
CLIP-IQA	0.164	0.513	0.700	0.083	0.363	0.653	0.025	0.096	0.241
META-IQA	-0.021	0.187	0.638	<u>-0.019</u>	<u>-0.015</u>	0.180	0.002	<u>0.003</u>	<u>0.007</u>
RANK-IQA	0.114	0.522	0.811	0.019	0.187	0.568	0.095	0.354	0.604
HYPER-IQA	<u>-0.137</u>	0.049	<u>0.237</u>	<b>-0.075</b>	<u>-0.074</u>	<u>0.079</u>	<b>-0.104</b>	0.043	0.289
KONCEPT	0.092	0.499	0.968	-0.014	0.248	0.627	0.144	0.489	0.841
FPR	0.816	1.945	4.502	0.329	0.862	1.684	0.392	1.091	2.928
NIMA	0.009	<u>0.019</u>	<u>0.089</u>	0.022	0.058	<u>0.110</u>	0.011	0.029	0.058
WSP	0.094	0.447	0.961	0.033	0.082	0.275	0.003	0.008	0.018
MDTVSFA	0.130	0.463	0.760	0.027	0.194	0.459	0.002	0.005	<u>0.010</u>
LINEARITY	0.243	0.724	1.284	-0.012	0.236	0.598	0.221	0.684	1.234
VSFA	0.161	0.686	1.513	0.029	0.188	0.506	0.003	0.012	0.042
PAQ2PIQ	0.170	0.781	1.374	0.012	0.176	0.671	0.139	0.705	1.287
SPAQ	<u>-0.079</u>	<u>0.030</u>	0.508	0.022	0.123	0.424	<u>-0.082</u>	<b>-0.045</b>	0.476
TRES	0.336	0.667	0.953	0.104	0.340	0.679	0.296	0.631	0.914
MANIQA	<b>-0.185</b>	<b>-0.394</b>	<b>-0.607</b>	<u>-0.062</u>	<b>-0.167</b>	<b>-0.301</b>	<u>-0.002</u>	<u>0.002</u>	<b>0.006</b>

VIMEO dataset, with domain transform, Energy score									
Attack Amplitude	Optimized-UAP			Generative-UAP			Cumulative-UAP		
	0.2	0.4	0.8	0.2	0.4	0.8	0.2	0.4	0.8
CLIP-IQA	0.173	0.678	0.811	0.006	0.445	0.765	0.019	0.059	0.175
META-IQA	-0.035	0.241	0.795	-0.026	-0.030	0.227	<u>0.002</u>	<u>0.004</u>	<u>0.008</u>
RANK-IQA	<u>-0.140</u>	0.248	0.604	<u>-0.063</u>	<u>-0.077</u>	0.267	0.019	0.137	0.367
HYPER-IQA	<u>-0.196</u>	<u>0.148</u>	<u>0.417</u>	<b>-0.114</b>	<u>-0.112</u>	<u>0.205</u>	<b>-0.130</b>	0.164	0.499
KONCEPT	0.071	0.519	1.034	-0.029	0.230	0.705	0.108	0.525	0.948
FPR	0.939	1.923	3.379	0.348	0.998	1.737	0.462	1.112	1.951
NIMA	-0.033	<u>-0.039</u>	<u>0.043</u>	0.021	0.054	<u>0.134</u>	0.007	0.018	0.035
WSP	0.254	0.970	1.629	0.083	0.204	0.578	0.004	0.014	0.039
MDTVSFA	0.490	0.899	1.042	0.085	0.475	0.799	<u>0.002</u>	<u>0.006</u>	<u>0.013</u>
LINEARITY	0.639	1.248	1.753	0.069	0.577	1.019	<u>0.583</u>	1.185	1.682
VSFA	0.512	1.510	2.469	0.077	0.508	1.075	0.004	0.018	0.052
PAQ2PIQ	0.318	1.072	1.559	-0.009	0.292	0.938	0.284	1.002	1.479
SPAQ	0.107	1.227	2.586	0.120	0.660	1.349	0.075	1.154	2.568
TRES	0.415	0.739	1.010	0.136	0.397	0.725	0.341	0.683	0.962
MANIQA	<b>-0.246</b>	<b>-0.491</b>	<b>-0.671</b>	<u>-0.087</u>	<b>-0.229</b>	<b>-0.428</b>	<u>-0.002</u>	<b>-0.006</b>	<b>-0.005</b>

"Blue sky" video from Derf's collection, with domain transform, Energy score									
Attack Amplitude	Optimized-UAP			Generative-UAP			Cumulative-UAP		
	0.2	0.4	0.8	0.2	0.4	0.8	0.2	0.4	0.8
CLIP-IQA	1.780	3.290	3.679	0.711	1.886	2.968	0.083	0.400	1.191
META-IQA	-0.318	-0.498	-0.671	-0.102	-0.242	-0.365	-0.009	-0.011	-0.018
RANK-IQA	-0.530	-0.621	0.277	-0.204	<u>-0.469</u>	<u>-0.762</u>	-0.137	<u>-0.317</u>	<u>-0.601</u>
HYPER-IQA	<b>-1.010</b>	<b>-1.511</b>	<b>-2.017</b>	<b>-0.397</b>	<b>-0.840</b>	<b>-1.243</b>	<b>-0.861</b>	<b>-1.337</b>	<b>-1.818</b>
KONCEPT	-0.342	-0.320	-0.170	-0.180	-0.292	-0.128	<u>-0.141</u>	0.168	0.466
FPR	1.625	3.194	5.420	0.476	1.700	3.079	0.790	1.670	2.606
NIMA	-0.236	-0.320	-0.501	<u>-0.215</u>	-0.294	-0.348	-0.045	-0.129	-0.247
WSP	1.699	2.948	3.565	0.267	0.832	1.993	0.038	0.104	0.218
MDTVSFA	1.381	2.062	2.222	0.162	0.785	1.525	0.007	0.007	0.019
LINEARITY	2.764	3.661	4.380	0.977	2.500	3.261	2.655	3.570	4.292
VSFA	2.930	5.229	7.133	0.392	2.331	3.966	-0.021	0.089	0.358
PAQ2PIQ	1.211	2.004	2.426	-0.008	1.002	1.795	1.083	1.872	2.281
SPAQ	<u>-0.568</u>	<u>-0.726</u>	<u>-0.875</u>	<u>-0.215</u>	-0.376	-0.300	<u>-0.577</u>	<u>-0.732</u>	<u>-0.871</u>
TRES	0.436	1.047	1.578	0.076	0.368	0.857	0.216	0.816	1.415
MANIQA	<u>-0.539</u>	<u>-1.168</u>	<u>-1.606</u>	-0.147	<u>-0.539</u>	<u>-1.137</u>	-0.009	-0.010	-0.062

Table 4: Robustness scores for tested metrics on different datasets. Table 1

NIPS 2017 dataset, with domain transform, Energy score						
Attack	FGSM	I-FGSM	MI-FGSM	AMI-FGSM	MADC	Korhonen et al.
CLIP-IQA	0.433	<b>0.795</b>	<b>0.780</b>	<b>0.780</b>	0.792	<u>0.787</u>
META-IQA	0.574	1.236	1.212	1.214	0.796	0.975
RANK-IQA	0.457	<u>1.145</u>	<u>0.967</u>	<u>0.968</u>	<b>0.448</b>	0.887
HYPER-IQA	<b>-0.290</b>	1.325	1.351	1.359	0.767	1.310
KONCEPT	0.557	1.200	1.014	1.014	0.670	1.001
FPR	0.947	3.389	3.274	3.276	1.523	3.179
NIMA	0.383	1.326	1.261	1.263	1.056	1.203
WSP	0.457	1.289	1.270	1.275	0.711	0.962
MDTVSFA	<u>0.259</u>	<u>0.938</u>	<u>0.902</u>	<u>0.902</u>	0.800	<b>0.762</b>
LINEARITY	<u>-0.158</u>	1.369	1.335	1.341	0.802	1.336
VSFA	0.404	2.091	2.276	2.275	1.347	1.579
PAQ2PIQ	0.658	1.282	1.212	1.216	<u>0.503</u>	1.088
SPAQ	0.294	1.452	1.332	1.336	<u>0.730</u>	1.318
TRES	0.807	1.206	1.188	1.190	0.668	1.164
MANIQA	0.530	1.331	1.166	1.167	<u>0.619</u>	<u>0.836</u>

VIMEO dataset, with domain transform, Energy score						
Attack	FGSM	I-FGSM	MI-FGSM	AMI-FGSM	MADC	Korhonen et al.
CLIP-IQA	0.411	<b>0.840</b>	<b>0.829</b>	<b>0.824</b>	0.833	<u>0.830</u>
META-IQA	0.544	1.402	1.379	1.379	1.059	1.101
RANK-IQA	0.196	<u>1.113</u>	<u>0.941</u>	<u>0.944</u>	<b>0.394</b>	<b>0.774</b>
HYPER-IQA	<b>-0.561</b>	1.496	1.538	1.552	0.979	1.472
KONCEPT	0.660	1.390	1.203	1.201	0.882	1.182
FPR	0.649	3.766	3.600	3.602	2.055	3.419
NIMA	0.183	1.197	1.143	1.142	0.966	1.026
WSP	0.485	1.404	1.381	1.385	0.871	1.026
MDTVSFA	<u>0.170</u>	<u>1.055</u>	<u>1.026</u>	<u>1.026</u>	0.976	<u>0.911</u>
LINEARITY	<u>-0.298</u>	1.388	1.325	1.325	0.927	1.304
VSFA	<u>0.321</u>	2.267	2.508	2.507	1.709	1.821
PAQ2PIQ	0.596	1.262	1.192	1.187	<u>0.589</u>	1.046
SPAQ	0.351	1.956	1.762	1.769	1.023	1.701
TRES	0.831	1.233	1.221	1.222	<u>0.763</u>	1.172
MANIQA	0.622	1.651	1.436	1.438	0.869	1.026

"Blue sky" video from Derf's collection, with domain transform, Energy score						
Attack	FGSM	I-FGSM	MI-FGSM	AMI-FGSM	MADC	Korhonen et al.
CLIP-IQA	2.016	3.719	3.764	3.642	3.643	3.531
META-IQA	1.086	2.372	2.308	2.321	1.662	<u>1.566</u>
RANK-IQA	1.119	<u>2.337</u>	<b>1.923</b>	<u>1.971</u>	<b>1.184</b>	1.749
HYPER-IQA	<b>0.428</b>	3.133	3.161	3.141	1.925	2.874
KONCEPT	1.345	2.530	<u>2.039</u>	<b>1.928</b>	1.504	1.785
FPR	2.044	8.405	8.212	8.173	4.463	6.615
NIMA	1.830	3.655	3.476	3.476	2.649	2.927
WSP	0.982	2.784	2.962	2.947	2.315	1.959
MDTVSFA	<u>0.547</u>	<u>2.295</u>	2.295	2.283	2.192	<b>1.218</b>
LINEARITY	1.060	3.684	3.355	3.369	2.894	3.335
VSFA	0.731	6.786	7.871	8.059	5.356	2.682
PAQ2PIQ	1.360	<b>2.247</b>	<u>2.179</u>	<u>2.171</u>	<u>1.324</u>	1.806
SPAQ	1.058	2.666	2.508	2.499	1.452	2.025
TRES	1.868	2.834	2.785	2.747	1.894	2.713
MANIQA	<u>0.559</u>	2.510	2.241	2.325	<u>1.377</u>	<u>1.239</u>

Table 5: Robustness scores for tested metrics on different datasets. Table 2

Attack Amplitude	Optimized-UAP			Generative-UAP			Cumulative-UAP		
	0.2	0.4	0.8	0.2	0.4	0.8	0.2	0.4	0.8
CLIP-IQA	0.107 (0.104, 0.110)	0.377 (0.371, 0.382)	0.456 (0.451, 0.462)	0.021 (0.018, 0.023)	0.240 (0.236, 0.243)	0.416 (0.412, 0.421)	0.011 (0.011, 0.012)	0.041 (0.040, 0.042)	0.116 (0.114, 0.118)
META-IQA	-0.020 (-0.022, -0.018)	0.110 (0.105, 0.115)	0.451 (0.442, 0.459)	-0.013 (-0.014, -0.013)	-0.016 (-0.018, -0.015)	0.104 (0.100, 0.108)	0.001 (0.001, 0.001)	0.001 (0.001, 0.002)	0.004 (0.003, 0.004)
RANK-IQA	-0.021 (-0.023, -0.019)	0.149 (0.145, 0.153)	0.342 (0.337, 0.347)	-0.018 (-0.019, -0.017)	0.014 (0.012, 0.016)	0.157 (0.153, 0.160)	0.014 (0.013, 0.015)	0.090 (0.088, 0.093)	0.192 (0.188, 0.196)
HYPER-IQA	-0.086 (-0.088, -0.084)	0.021 (0.017, 0.025)	0.149 (0.143, 0.155)	<b>-0.052</b> (-0.053, -0.051)	-0.046 (-0.048, -0.045)	0.065 (0.061, 0.069)	<b>-0.057</b> (-0.059, -0.056)	0.037 (0.034, 0.041)	0.191 (0.185, 0.197)
KONCEPT	0.030 (0.028, 0.032)	0.241 (0.236, 0.246)	0.594 (0.586, 0.601)	-0.011 (-0.012, -0.010)	0.104 (0.101, 0.108)	0.342 (0.337, 0.348)	0.052 (0.049, 0.054)	0.245 (0.241, 0.250)	0.501 (0.495, 0.506)
FPR	0.621 (0.606, 0.636)	2.502 (2.452, 2.552)	7.970 (7.833, 8.107)	0.146 (0.143, 0.149)	0.665 (0.652, 0.679)	1.836 (1.807, 1.865)	0.218 (0.211, 0.224)	1.093 (1.059, 1.127)	3.657 (3.556, 3.759)
NIMA	-0.010 (-0.012, -0.009)	-0.008 (-0.011, -0.006)	0.022 (0.019, 0.025)	0.005 (0.004, 0.006)	0.022 (0.021, 0.024)	0.057 (0.055, 0.06)	0.004 (0.003, 0.004)	0.011 (0.010, 0.012)	0.021 (0.019, 0.022)
WSP	0.129 (0.125, 0.134)	0.595 (0.585, 0.606)	1.288 (1.273, 1.302)	0.033 (0.032, 0.034)	0.086 (0.084, 0.088)	0.269 (0.264, 0.275)	0.002 (0.002, 0.002)	0.006 (0.006, 0.007)	0.017 (0.016, 0.017)
MDTVSEA	0.216 (0.211, 0.222)	0.461 (0.455, 0.467)	0.586 (0.581, 0.591)	0.034 (0.032, 0.035)	0.201 (0.197, 0.205)	0.380 (0.375, 0.385)	0.001 (0.001, 0.001)	0.003 (0.002, 0.003)	0.006 (0.005, 0.006)
LINEARITY	0.333 (0.325, 0.340)	0.859 (0.847, 0.871)	1.500 (1.486, 1.513)	0.032 (0.030, 0.034)	0.281 (0.275, 0.287)	0.591 (0.583, 0.599)	0.296 (0.289, 0.303)	0.786 (0.775, 0.798)	1.393 (1.380, 1.406)
VSFA	0.281 (0.273, 0.290)	1.247 (1.225, 1.269)	2.622 (2.597, 2.647)	0.030 (0.028, 0.032)	0.246 (0.240, 0.252)	0.662 (0.651, 0.672)	0.002 (0.001, 0.002)	0.008 (0.007, 0.008)	0.025 (0.024, 0.027)
PAQ2PIQ	0.161 (0.156, 0.165)	0.662 (0.654, 0.671)	1.204 (1.195, 1.213)	-0.000 (-0.001, 0.000)	0.136 (0.132, 0.139)	0.520 (0.514, 0.527)	0.136 (0.132, 0.140)	0.581 (0.574, 0.589)	1.088 (1.080, 1.097)
SPAQ	0.007 (0.005, 0.010)	0.519 (0.503, 0.534)	1.797 (1.761, 1.832)	0.030 (0.029, 0.031)	0.206 (0.200, 0.212)	0.580 (0.569, 0.591)	-0.002 (-0.005, -0.0)	0.462 (0.448, 0.477)	1.772 (1.736, 1.807)
TRES	0.203 (0.200, 0.206)	0.403 (0.399, 0.407)	0.631 (0.626, 0.635)	0.065 (0.064, 0.066)	0.197 (0.194, 0.200)	0.392 (0.388, 0.395)	0.169 (0.167, 0.171)	0.366 (0.362, 0.369)	0.589 (0.584, 0.594)
MANIQA	<b>-0.107</b> (-0.108, -0.106)	<b>-0.221</b> (-0.223, -0.219)	<b>-0.318</b> (-0.322, -0.315)	<b>-0.037</b> (-0.037, -0.036)	<b>-0.099</b> (-0.1, -0.098)	<b>-0.187</b> (-0.189, -0.184)	<b>-0.0</b> (-0.0, -0.0)	<b>-0.002</b> (-0.002, -0.001)	<b>-0.001</b> (-0.001, -0.0)

Table 6: All datasets, with domain transform, Abs. gain. Table 1

Attack	FGSM	I-FGSM	MI-FGSM	AMI-FGSM	MADC	Korhonen et al.
CLIP-IQA	0.243 (0.239, 0.248)	<b>0.484</b> (0.476, 0.492)	<b>0.474</b> (0.467, 0.482)	<b>0.471</b> (0.464, 0.479)	0.477 (0.469, 0.485)	<u>0.47</u> (0.463, 0.478)
META-IQA	0.334 (0.328, 0.341)	0.975 (0.968, 0.982)	0.950 (0.943, 0.957)	0.952 (0.945, 0.959)	0.638 (0.632, 0.644)	0.710 (0.704, 0.716)
RANK-IQA	0.142 (0.136, 0.149)	<u>0.712</u> (0.707, 0.716)	<u>0.558</u> (0.555, 0.562)	<u>0.561</u> (0.557, 0.564)	<b>0.197</b> (0.195, 0.2)	<b>0.43</b> (0.425, 0.435)
HYPER-IQA	<b>-0.242</b> (-0.251, -0.234)	1.210 (1.199, 1.221)	1.247 (1.236, 1.258)	1.262 (1.251, 1.273)	0.521 (0.515, 0.526)	1.157 (1.147, 1.168)
KONCEPT	0.314 (0.311, 0.318)	0.940 (0.935, 0.945)	0.701 (0.697, 0.706)	0.702 (0.697, 0.706)	0.416 (0.412, 0.420)	0.671 (0.666, 0.676)
FPR	0.490 (0.478, 0.503)	6.078 (6.052, 6.104)	5.713 (5.683, 5.742)	5.724 (5.695, 5.753)	1.864 (1.840, 1.888)	5.246 (5.207, 5.284)
NIMA	0.133 (0.128, 0.138)	0.846 (0.839, 0.852)	0.777 (0.770, 0.783)	0.776 (0.770, 0.783)	0.637 (0.630, 0.645)	0.699 (0.691, 0.707)
WSP	0.241 (0.238, 0.244)	1.011 (1.004, 1.017)	1.005 (0.999, 1.012)	1.014 (1.007, 1.020)	0.467 (0.462, 0.472)	0.619 (0.614, 0.625)
MDTVSFA	<u>0.101</u> (0.095, 0.106)	<u>0.624</u> (0.618, 0.631)	<u>0.596</u> (0.59, 0.602)	<u>0.596</u> (0.59, 0.602)	0.543 (0.537, 0.549)	<u>0.467</u> (0.462, 0.473)
LINEARITY	<u>-0.098</u> (-0.103, -0.092)	1.019 (1.013, 1.024)	0.951 (0.947, 0.955)	0.959 (0.955, 0.963)	0.516 (0.511, 0.521)	0.941 (0.936, 0.945)
VSFA	0.173 (0.168, 0.178)	2.439 (2.428, 2.451)	2.901 (2.890, 2.912)	2.905 (2.894, 2.917)	1.392 (1.382, 1.403)	1.596 (1.579, 1.614)
PAQ2PIQ	0.319 (0.315, 0.322)	0.860 (0.852, 0.868)	0.782 (0.774, 0.789)	0.783 (0.776, 0.791)	<u>0.274</u> (0.269, 0.278)	0.640 (0.635, 0.646)
SPAQ	0.163 (0.159, 0.167)	1.374 (1.366, 1.381)	1.171 (1.164, 1.177)	1.176 (1.169, 1.183)	0.476 (0.472, 0.481)	1.092 (1.085, 1.099)
TRES	0.479 (0.474, 0.485)	0.903 (0.897, 0.909)	0.878 (0.872, 0.884)	0.880 (0.874, 0.886)	0.448 (0.444, 0.453)	0.848 (0.842, 0.855)
MANIQA	0.295 (0.290, 0.299)	1.325 (1.305, 1.344)	0.939 (0.930, 0.948)	0.942 (0.932, 0.951)	<u>0.412</u> (0.408, 0.416)	0.529 (0.524, 0.535)

Table 7: All datasets, with domain transform, Abs. gain. Table 2

Attack	Optimized-UAP			Generative-UAP			Cumulative-UAP		
	0.2	0.4	0.8	0.2	0.4	0.8	0.2	0.4	0.8
Amplitude	0.078	0.272	0.329	0.017	0.169	0.298	0.008	0.028	0.081
CLIP-IQA	(0.076, 0.080)	(0.268, 0.277)	(0.324, 0.334)	(0.015, 0.019)	(0.166, 0.172)	(0.294, 0.303)	(0.007, 0.008)	(0.027, 0.029)	(0.080, 0.083)
META-IQA	<u>-0.013</u>	0.087	0.342	-0.009	<u>-0.01</u>	0.081	<u>0.0</u>	<u>0.001</u>	<u>0.003</u>
	(-0.014, -0.011)	(0.083, 0.091)	(0.335, 0.349)	(-0.010, -0.009)	(-0.012, -0.009)	(0.078, 0.085)	(0.0, 0.001)	(0.001, 0.001)	(0.002, 0.003)
RANK-IQA	-0.009	0.101	0.221	<u>-0.01</u>	0.013	0.106	0.010	0.061	0.128
	(-0.010, -0.007)	(0.098, 0.103)	(0.218, 0.225)	(-0.011, -0.01)	(0.012, 0.015)	(0.103, 0.109)	(0.010, 0.011)	(0.059, 0.063)	(0.125, 0.131)
HYPER-IQA	<u>-0.052</u>	<u>0.022</u>	<u>0.105</u>	<b>-0.033</b>	<u>-0.027</u>	<u>0.05</u>	<b>-0.034</b>	0.032	0.132
	(-0.054, -0.051)	(0.019, 0.025)	(0.1, 0.109)	(-0.034, -0.032)	(-0.028, -0.026)	(0.047, 0.053)	(-0.036, -0.033)	(0.029, 0.035)	(0.127, 0.137)
KONCEPT	0.023	0.170	0.410	-0.007	0.074	0.239	0.037	0.172	0.347
	(0.021, 0.025)	(0.166, 0.173)	(0.404, 0.415)	(-0.007, -0.006)	(0.072, 0.077)	(0.235, 0.243)	(0.036, 0.039)	(0.168, 0.176)	(0.342, 0.351)
FPR	0.435	1.717	5.305	0.102	0.463	1.250	0.153	0.765	2.441
	(0.423, 0.448)	(1.679, 1.755)	(5.209, 5.402)	(0.099, 0.104)	(0.452, 0.474)	(1.227, 1.272)	(0.148, 0.159)	(0.739, 0.791)	(2.372, 2.511)
NIMA	-0.005	-0.003	<u>0.018</u>	0.004	0.017	0.041	0.003	0.008	0.015
	(-0.006, -0.004)	(-0.005, -0.002)	(0.016, 0.02)	(0.004, 0.005)	(0.016, 0.018)	(0.039, 0.043)	(0.002, 0.003)	(0.007, 0.008)	(0.014, 0.016)
WSP	0.100	0.445	0.940	0.025	0.065	0.205	0.001	0.005	0.012
	(0.097, 0.104)	(0.436, 0.454)	(0.927, 0.953)	(0.024, 0.025)	(0.063, 0.067)	(0.200, 0.209)	(0.001, 0.001)	(0.004, 0.005)	(0.012, 0.013)
MDTVSFA	0.149	0.309	0.388	0.023	0.135	0.254	0.001	0.002	0.004
	(0.145, 0.153)	(0.304, 0.314)	(0.384, 0.393)	(0.022, 0.024)	(0.132, 0.138)	(0.250, 0.258)	(0.001, 0.001)	(0.002, 0.002)	(0.004, 0.004)
LINEARITY	0.229	0.567	0.970	0.024	0.192	0.393	0.204	0.520	0.903
	(0.223, 0.235)	(0.558, 0.577)	(0.960, 0.981)	(0.023, 0.026)	(0.188, 0.197)	(0.386, 0.399)	(0.199, 0.210)	(0.512, 0.529)	(0.893, 0.914)
VSFA	0.201	0.862	1.784	0.021	0.174	0.460	0.001	0.005	0.018
	(0.195, 0.208)	(0.846, 0.878)	(1.766, 1.803)	(0.020, 0.022)	(0.169, 0.178)	(0.452, 0.468)	(0.001, 0.001)	(0.005, 0.006)	(0.017, 0.019)
PAQ2PIQ	0.111	0.435	0.778	-0.000	0.093	0.345	0.094	0.384	0.703
	(0.108, 0.115)	(0.428, 0.442)	(0.770, 0.786)	(-0.000, 0.000)	(0.090, 0.096)	(0.339, 0.350)	(0.091, 0.098)	(0.377, 0.390)	(0.695, 0.710)
SPAQ	0.010	0.438	1.458	0.025	0.173	0.472	0.002	0.392	1.439
	(0.008, 0.012)	(0.425, 0.452)	(1.427, 1.489)	(0.024, 0.026)	(0.168, 0.179)	(0.462, 0.482)	(0.000, 0.004)	(0.379, 0.405)	(1.408, 1.471)
TRES	0.144	0.288	0.445	0.046	0.140	0.279	0.120	0.260	0.416
	(0.142, 0.147)	(0.284, 0.291)	(0.441, 0.450)	(0.045, 0.046)	(0.138, 0.142)	(0.275, 0.283)	(0.118, 0.122)	(0.257, 0.264)	(0.412, 0.420)
MANIQA	<b>-0.074</b>	<b>-0.151</b>	<b>-0.214</b>	<u>-0.026</u>	<b>-0.069</b>	<b>-0.128</b>	<u>-0.0</u>	<b>-0.001</b>	<b>-0.001</b>
	(-0.075, -0.073)	(-0.152, -0.15)	(-0.216, -0.212)	(-0.026, -0.025)	(-0.07, -0.068)	(-0.129, -0.126)	(-0.0, -0.0)	(-0.001, -0.001)	(-0.001, -0.0)

Table 8: All datasets, with domain transform, Rel. gain. Table 1



Attack	FGSM	I-FGSM	MI-FGSM	AMI-FGSM	MADC	Korhonen et al.
CLIP-IQA	0.171 (0.167, 0.175)	<b>0.35</b> (0.342, 0.358)	<b>0.344</b> (0.336, 0.351)	<b>0.341</b> (0.334, 0.349)	0.344 (0.337, 0.352)	0.339 (0.332, 0.347)
META-IQA	0.251 (0.245, 0.256)	0.736 (0.727, 0.744)	0.716 (0.708, 0.725)	0.718 (0.710, 0.727)	0.478 (0.472, 0.484)	0.529 (0.523, 0.536)
RANK-IQA	0.100 (0.095, 0.104)	<u>0.45</u> (0.445, 0.455)	<u>0.352</u> (0.348, 0.356)	<u>0.354</u> (0.35, 0.357)	<b>0.128</b> (0.125, 0.13)	<b>0.276</b> (0.272, 0.281)
HYPER-IQA	<b>-0.146</b> (-0.152, -0.141)	0.758 (0.750, 0.766)	0.784 (0.776, 0.792)	0.791 (0.783, 0.799)	0.335 (0.330, 0.340)	0.728 (0.721, 0.736)
KONCEPT	0.215 (0.212, 0.218)	0.636 (0.631, 0.642)	0.478 (0.473, 0.482)	0.478 (0.473, 0.483)	<u>0.287</u> (0.283, 0.291)	0.459 (0.454, 0.463)
FPR	0.307 (0.300, 0.315)	3.986 (3.961, 4.011)	3.737 (3.714, 3.761)	3.746 (3.723, 3.770)	1.258 (1.237, 1.279)	3.444 (3.414, 3.474)
NIMA	0.093 (0.089, 0.097)	0.564 (0.557, 0.571)	0.517 (0.511, 0.524)	0.517 (0.511, 0.524)	0.425 (0.418, 0.432)	0.468 (0.461, 0.475)
WSP	0.171 (0.168, 0.174)	0.714 (0.707, 0.721)	0.709 (0.702, 0.715)	0.716 (0.709, 0.723)	0.337 (0.332, 0.342)	0.439 (0.434, 0.445)
MDTVSFA	0.069 (0.065, 0.073)	<u>0.412</u> (0.406, 0.418)	<u>0.394</u> (0.388, 0.401)	<u>0.394</u> (0.388, 0.4)	0.360 (0.354, 0.366)	<u>0.307</u> (0.302, 0.312)
LINEARITY	-0.055 (-0.058, -0.052)	0.651 (0.645, 0.657)	0.604 (0.600, 0.609)	0.608 (0.604, 0.613)	0.336 (0.331, 0.340)	0.598 (0.593, 0.603)
VSFA	0.117 (0.114, 0.121)	1.643 (1.633, 1.654)	1.959 (1.946, 1.972)	1.963 (1.950, 1.975)	0.943 (0.934, 0.952)	1.055 (1.043, 1.066)
PAQ2PIQ	0.206 (0.202, 0.209)	0.554 (0.546, 0.562)	0.504 (0.496, 0.511)	0.504 (0.497, 0.511)	<u>0.18</u> (0.176, 0.184)	0.411 (0.406, 0.417)
SPAQ	0.120 (0.117, 0.123)	1.038 (1.029, 1.047)	0.882 (0.874, 0.889)	0.885 (0.878, 0.893)	0.364 (0.359, 0.369)	0.821 (0.814, 0.828)
TRES	0.343 (0.338, 0.348)	0.632 (0.625, 0.639)	0.613 (0.607, 0.620)	0.615 (0.609, 0.622)	0.315 (0.311, 0.320)	0.596 (0.589, 0.602)
MANIQA	0.215 (0.211, 0.219)	0.954 (0.938, 0.970)	0.678 (0.669, 0.687)	0.680 (0.671, 0.689)	0.299 (0.295, 0.303)	0.385 (0.380, 0.390)

Table 9: All datasets, with domain transform, Rel. gain. Table 2

Attack Amplitude	Optimized-UAP			Generative-UAP			Cumulative-UAP		
	0.2	0.4	0.8	0.2	0.4	0.8	0.2	0.4	0.8
CLIP-IQA	0.948 (0.935, 0.961)	0.359 (0.350, 0.368)	0.242 (0.235, 0.249)	1.144 (1.130, 1.157)	0.555 (0.545, 0.564)	0.274 (0.267, 0.281)	1.840 (1.826, 1.854)	1.331 (1.318, 1.343)	0.897 (0.886, 0.908)
META-IQA	1.305 (1.291, 1.319)	0.871 (0.857, 0.884)	0.299 (0.289, 0.310)	1.723 (1.709, 1.737)	1.376 (1.363, 1.39)	0.918 (0.904, 0.932)	2.641 (2.625, 2.657)	2.517 (2.502, 2.532)	<b>2.332</b> (2.318, 2.347)
RANK-IQA	1.152 (1.140, 1.163)	0.812 (0.799, 0.826)	<u>0.381</u> (0.372, 0.39)	1.556 (1.544, 1.568)	<u>1.207</u> (1.195, 1.22)	0.780 (0.767, 0.793)	1.653 (1.639, 1.667)	1.086 (1.071, 1.100)	0.652 (0.641, 0.662)
HYPER-IQA	0.996 (0.984, 1.007)	<u>1.007</u> (0.994, 1.02)	<u>0.692</u> (0.678, 0.705)	1.282 (1.270, 1.294)	1.188 (1.175, 1.200)	<u>1.014</u> (0.999, 1.028)	1.149 (1.137, 1.160)	1.055 (1.042, 1.069)	0.632 (0.619, 0.645)
KONCEPT	1.219 (1.206, 1.233)	0.567 (0.555, 0.579)	0.121 (0.111, 0.131)	1.546 (1.534, 1.559)	0.991 (0.977, 1.006)	0.412 (0.400, 0.424)	1.266 (1.252, 1.281)	0.574 (0.562, 0.586)	0.166 (0.158, 0.174)
FPR	0.155 (0.145, 0.164)	-0.478 (-0.487, -0.469)	-1.019 (-1.026, -1.012)	0.791 (0.781, 0.801)	0.111 (0.102, 0.121)	-0.380 (-0.388, -0.373)	0.648 (0.637, 0.659)	0.004 (-0.008, 0.016)	-0.569 (-0.579, -0.558)
NIMA	<b>1.413</b> (1.4, 1.426)	<b>1.243</b> (1.23, 1.256)	<b>1.115</b> (1.103, 1.128)	<u>1.63</u> (1.616, 1.644)	<b>1.381</b> (1.368, 1.395)	<b>1.141</b> (1.128, 1.155)	2.188 (2.173, 2.204)	1.859 (1.844, 1.875)	1.574 (1.559, 1.589)
WSP	0.998 (0.983, 1.013)	0.239 (0.225, 0.252)	-0.211 (-0.220, -0.203)	1.517 (1.504, 1.531)	1.117 (1.103, 1.130)	0.575 (0.562, 0.587)	2.404 (2.390, 2.417)	2.157 (2.143, 2.171)	1.834 (1.820, 1.849)
MDTVSFA	0.706 (0.691, 0.721)	0.267 (0.256, 0.277)	0.094 (0.088, 0.100)	1.396 (1.382, 1.411)	0.735 (0.721, 0.749)	0.337 (0.327, 0.347)	<b>2.853</b> (2.839, 2.866)	<b>2.581</b> (2.566, 2.595)	<u>2.267</u> (2.253, 2.282)
LINEARITY	0.586 (0.570, 0.602)	0.035 (0.023, 0.046)	-0.293 (-0.300, -0.287)	1.393 (1.379, 1.408)	0.647 (0.631, 0.662)	0.190 (0.179, 0.202)	0.648 (0.632, 0.664)	0.078 (0.066, 0.089)	-0.260 (-0.267, -0.254)
VSFA	0.646 (0.631, 0.662)	-0.094 (-0.107, -0.081)	-0.555 (-0.561, -0.548)	1.364 (1.350, 1.378)	0.675 (0.660, 0.689)	0.139 (0.128, 0.150)	2.512 (2.498, 2.526)	2.241 (2.225, 2.257)	1.890 (1.872, 1.908)
PAQ2PIQ	0.986 (0.969, 1.003)	0.101 (0.092, 0.110)	-0.229 (-0.233, -0.224)	<b>1.972</b> (1.958, 1.985)	0.986 (0.971, 1.002)	0.203 (0.194, 0.211)	1.045 (1.028, 1.062)	0.161 (0.152, 0.171)	-0.181 (-0.186, -0.176)
SPAQ	<u>1.314</u> (1.3, 1.327)	0.409 (0.394, 0.424)	-0.160 (-0.175, -0.145)	1.584 (1.570, 1.599)	0.829 (0.814, 0.844)	0.292 (0.279, 0.306)	1.356 (1.343, 1.370)	0.447 (0.432, 0.462)	-0.144 (-0.159, -0.129)
TRES	0.586 (0.578, 0.594)	0.247 (0.242, 0.252)	0.031 (0.028, 0.035)	1.110 (1.100, 1.119)	0.604 (0.595, 0.612)	0.265 (0.260, 0.271)	0.684 (0.675, 0.693)	0.300 (0.294, 0.306)	0.066 (0.062, 0.070)
MANIQA	0.861 (0.853, 0.870)	0.524 (0.517, 0.531)	0.374 (0.365, 0.383)	1.359 (1.349, 1.368)	0.900 (0.892, 0.909)	0.622 (0.613, 0.631)	<u>2.532</u> (2.52, 2.545)	<u>2.405</u> (2.392, 2.418)	<u>2.158</u> (2.144, 2.172)

Table 10: All datasets, with domain transform, Robustness score. Table 1

Attack	FGSM	I-FGSM	MI-FGSM	AMI-FGSM	MADC	Korhonen et al.
CLIP-IQA	0.532 (0.520, 0.544)	<b>0.21</b> (0.201, 0.219)	<b>0.219</b> (0.21, 0.229)	<b>0.221</b> (0.212, 0.231)	0.216 (0.206, 0.225)	<b>0.22</b> (0.21, 0.229)
META-IQA	0.400 (0.387, 0.412)	-0.140 (-0.144, -0.137)	-0.129 (-0.132, -0.125)	-0.130 (-0.133, -0.126)	0.048 (0.044, 0.053)	0.002 (-0.003, 0.006)
RANK-IQA	0.712 (0.695, 0.730)	<u>-0.019</u> (-0.023, -0.014)	<u>0.085</u> (0.081, 0.089)	<u>0.083</u> (0.079, 0.087)	<b>0.567</b> (0.559, 0.575)	<u>0.219</u> (0.212, 0.226)
HYPER-IQA	0.579 (0.560, 0.597)	-0.243 (-0.247, -0.239)	-0.262 (-0.266, -0.258)	-0.265 (-0.269, -0.260)	0.128 (0.122, 0.134)	-0.226 (-0.230, -0.221)
KONCEPT	0.328 (0.321, 0.335)	-0.173 (-0.176, -0.170)	-0.045 (-0.049, -0.041)	-0.045 (-0.049, -0.041)	0.194 (0.189, 0.200)	-0.023 (-0.027, -0.019)
FPR	0.195 (0.180, 0.209)	-0.988 (-0.991, -0.985)	-0.960 (-0.963, -0.957)	-0.961 (-0.965, -0.958)	-0.446 (-0.453, -0.440)	-0.917 (-0.921, -0.913)
NIMA	<u>0.769</u> (0.752, 0.786)	-0.114 (-0.119, -0.109)	-0.076 (-0.080, -0.071)	-0.076 (-0.081, -0.071)	0.027 (0.020, 0.033)	-0.015 (-0.022, -0.008)
WSP	0.472 (0.464, 0.480)	-0.182 (-0.186, -0.178)	-0.180 (-0.183, -0.176)	-0.183 (-0.187, -0.179)	0.166 (0.162, 0.171)	0.040 (0.035, 0.045)
MDTVSFA	<b>0.808</b> (0.791, 0.825)	<u>0.045</u> (0.039, 0.051)	<u>0.067</u> (0.061, 0.073)	<u>0.067</u> (0.061, 0.073)	0.113 (0.106, 0.120)	<u>0.18</u> (0.173, 0.188)
LINEARITY	<u>0.786</u> (0.771, 0.801)	-0.165 (-0.169, -0.161)	-0.137 (-0.141, -0.134)	-0.140 (-0.144, -0.136)	0.143 (0.138, 0.149)	-0.130 (-0.134, -0.126)
VSFA	0.698 (0.681, 0.716)	-0.573 (-0.576, -0.569)	-0.649 (-0.652, -0.645)	-0.650 (-0.653, -0.646)	-0.320 (-0.325, -0.316)	-0.359 (-0.367, -0.350)
PAQ2PIQ	0.351 (0.346, 0.357)	-0.091 (-0.096, -0.087)	-0.051 (-0.055, -0.046)	-0.051 (-0.055, -0.046)	<u>0.428</u> (0.421, 0.435)	0.034 (0.030, 0.039)
SPAQ	0.718 (0.703, 0.733)	-0.296 (-0.300, -0.293)	-0.227 (-0.230, -0.224)	-0.229 (-0.233, -0.226)	0.177 (0.172, 0.182)	-0.195 (-0.199, -0.192)
TRES	0.163 (0.156, 0.171)	-0.136 (-0.140, -0.132)	-0.125 (-0.129, -0.120)	-0.125 (-0.130, -0.121)	0.180 (0.174, 0.186)	-0.106 (-0.110, -0.101)
MANIQA	0.409 (0.399, 0.419)	-0.277 (-0.283, -0.272)	-0.143 (-0.147, -0.139)	-0.144 (-0.148, -0.140)	<u>0.219</u> (0.215, 0.224)	0.115 (0.110, 0.121)

Table 11: All datasets, with domain transform, Robustness score. Table 2

Attack Amplitude	Optimized-UAP			Generative-UAP			Cumulative-UAP		
	0.2	0.4	0.8	0.2	0.4	0.8	0.2	0.4	0.8
CLIP-IQA	0.107	0.377	0.456	0.021	0.240	0.416	0.011	0.041	0.116
META-IQA	-0.020	0.110	0.451	-0.013	<u>-0.016</u>	0.104	0.001	<u>0.001</u>	<u>0.004</u>
RANK-IQA	<u>-0.041</u>	0.149	0.342	<u>-0.020</u>	0.035	0.157	0.017	0.090	0.192
HYPER-IQA	<u>-0.086</u>	<u>0.035</u>	<u>0.155</u>	<b>-0.052</b>	<u>-0.048</u>	<u>0.065</u>	<b>-0.058</b>	0.040	0.193
KONCEPT	0.030	0.241	0.594	-0.011	0.104	0.342	0.052	0.245	0.501
FPR	0.621	2.502	7.970	0.146	0.665	1.836	0.218	1.093	3.657
NIMA	-0.012	<u>-0.011</u>	<u>0.024</u>	0.009	0.025	<u>0.057</u>	0.004	0.011	0.021
WSP	0.129	0.595	1.288	0.033	0.086	0.269	0.002	0.006	0.017
MDTVSFA	0.216	0.461	0.586	0.034	0.201	0.380	0.001	<u>0.003</u>	<u>0.006</u>
LINEARITY	0.333	0.859	1.500	0.032	0.281	0.591	0.296	0.786	1.393
VSFA	0.281	1.247	2.622	0.030	0.246	0.662	0.002	0.008	0.025
PAQ2PIQ	0.161	0.662	1.204	-0.003	0.136	0.520	0.136	0.581	1.088
SPAQ	0.017	0.519	1.797	0.030	0.206	0.580	<u>-0.013</u>	0.462	1.772
TRES	0.203	0.403	0.631	0.065	0.197	0.392	0.169	0.366	0.589
MANIQA	<b>-0.107</b>	<b>-0.221</b>	<b>-0.318</b>	<u>-0.037</u>	<b>-0.099</b>	<b>-0.187</b>	<u>-0.001</u>	<b>-0.002</b>	<b>-0.002</b>

Table 12: All datasets, with domain transform, Wasserstein score. Table 1

Attack FGSM	I-FGSM	MI-FGSM	AMI-FGSM	MADC	Korhonen et al.
CLIP-IQA	0.243	<b>0.484</b>	<b>0.474</b>	<b>0.471</b>	0.477
META-IQA	0.334	0.975	0.950	0.952	0.638
RANK-IQA	0.142	<u>0.712</u>	<u>0.558</u>	<u>0.561</u>	<b>0.197</b>
HYPER-IQA	<b>-0.243</b>	1.210	1.247	1.262	0.521
KONCEPT	0.314	0.940	0.701	0.702	0.416
FPR	0.496	6.078	5.713	5.724	1.864
NIMA	0.133	0.846	0.777	0.776	0.637
WSP	0.241	1.011	1.005	1.014	0.467
MDTVSFA	<u>0.101</u>	<u>0.624</u>	<u>0.596</u>	<u>0.596</u>	0.543
LINEARITY	<u>-0.113</u>	1.019	0.951	0.959	0.516
VSFA	0.173	2.439	2.901	2.905	1.392
PAQ2PIQ	0.319	0.860	0.782	0.783	<u>0.274</u>
SPAQ	0.163	1.374	1.171	1.176	0.476
TRES	0.479	0.903	0.878	0.880	0.448
MANIQA	0.295	1.325	0.939	0.942	<u>0.412</u>

Table 13: All datasets, with domain transform, Wasserstein score. Table 2

metric	Cumulative-UAP		Generative-UAP		Optimized-UAP	
	COCO	Pascal VOC 2012	COCO	Pascal VOC 2012	COCO	Pascal VOC 2012
CLIP-IQA	0.059	0.076	0.473	0.326	0.643	0.623
META-IQA	<u>0.003</u>	<u>0.003</u>	<u>-0.027</u>	<u>-0.031</u>	0.210	0.157
RANK-IQA	0.147	0.216	0.066	0.063	0.301	0.289
HYPER-IQA	0.108	0.074	<u>-0.092</u>	<u>-0.097</u>	<u>0.083</u>	<u>0.069</u>
KONCEPT	0.447	0.424	0.179	0.194	0.434	0.406
FPR	0.923	1.013	0.859	0.834	1.688	1.726
NIMA	0.014	0.023	0.030	0.065	<u>-0.022</u>	<u>-0.027</u>
WSP	0.006	0.018	0.126	0.184	<u>0.775</u>	<u>0.798</u>
MDTVSFA	<u>0.004</u>	<u>0.006</u>	0.319	0.404	0.756	0.755
LINEARITY	0.975	0.971	0.420	0.472	1.004	1.043
VSFA	<u>0.004</u>	0.024	0.330	0.394	1.174	1.130
PAQ2PIQ	<u>0.866</u>	0.883	0.234	0.270	0.948	0.941
SPAQ	0.568	0.551	0.406	0.313	0.647	0.564
TRES	0.627	0.643	0.358	0.359	0.697	0.686
MANIQA	<b>-0.002</b>	<b>-0.005</b>	<b>-0.170</b>	<b>-0.179</b>	<b>-0.398</b>	<b>-0.382</b>

Table 14: All datasets, with domain transform, Energy score, UAP attacks by dataset.

Score Metric	<i>Abs.gain</i> ↓	<i>Rel.gain</i> ↓	<i>R<sub>score</sub></i> ↑	<i>E<sub>score</sub></i> ↓	<i>W<sub>score</sub></i> ↓
CLIP-IQA	0.272(0.270, 0.274)	0.200(0.199, 0.202)	0.705(0.700, 0.710)	0.440	0.272
META-IQA	0.263(0.260, 0.266)	0.206(0.204, 0.208)	<b>1.311(1.302, 1.319)</b>	0.344	0.263
RANK-IQA	0.190(0.188, 0.192)	0.125(0.124, 0.127)	0.811(0.806, 0.815)	0.295	<u>0.190</u>
HYPER-IQA	<u>0.196(0.193, 0.199)</u>	<u>0.117(0.116, 0.119)</u>	0.874(0.869, 0.879)	<u>0.253</u>	0.199
KONCEPT	0.353(0.350, 0.355)	<u>0.241(0.240, 0.243)</u>	0.608(0.602, 0.613)	0.495	0.353
FPR	2.874(2.846, 2.903)	1.775(1.758, 1.793)	-0.165(-0.170, -0.160)	1.424	2.874
NIMA	0.139(0.137, 0.141)	0.092(0.091, 0.094)	1.167(1.161, 1.172)	<u>0.215</u>	<b>0.139</b>
WSP	<u>0.332(0.329, 0.335)</u>	<u>0.221(0.219, 0.223)</u>	<u>1.018(1.011, 1.026)</u>	0.416	0.332
MDTVSFA	0.338(0.336, 0.340)	0.230(0.228, 0.231)	0.953(0.945, 0.962)	0.494	0.338
LINEARITY	0.705(0.700, 0.709)	0.452(0.449, 0.455)	0.281(0.276, 0.286)	0.783	0.705
VSFA	0.724(0.718, 0.730)	0.474(0.470, 0.478)	0.766(0.757, 0.775)	0.675	0.724
PAQ2PIQ	0.504(0.501, 0.508)	0.318(0.315, 0.320)	0.516(0.511, 0.522)	0.650	0.504
SPAQ	0.664(0.658, 0.671)	0.504(0.499, 0.509)	0.500(0.494, 0.506)	0.632	0.664
TRES	0.555(0.552, 0.558)	0.427(0.425, 0.430)	0.295(0.292, 0.299)	0.705	0.555
MANIQA	<b>0.110(0.107, 0.114)</b>	<b>0.078(0.075, 0.080)</b>	<u>1.110(1.102, 1.118)</u>	<b>0.206</b>	<u>0.175</u>

Table 15: All datasets, all scores, without domain transform.

Metric	CLIP-IQA	META-IQA	RANK-IQA	HYPER-IQA	KONCEPT	FPR	NIMA	WSP	MDTVSFA	LINEARITY	VSFA	PAQ2PIQ	SPAQ	TRES	MANIQA
CLIP-IQA	-	-1, 1, 1, 1, -1	-1, 1, -1, -1, -1	-1, 1, 1, 1, -1	1, 1, 1, -1, 1	1, 1, 1, 1, 1	-1, 1, 1, 1, -1	1, 1, 1, -1, -1	1, 1, -1, 1, -1	1, 1, 1, 1, 1	1, 1, 1, 1, 1	1, 1, 1, -1, 1	1, 1, 1, -1, 1	1, 1, 1, -1, 1	-1, 1, 1, -1, -1
META-IQA	1, -1, -1, -1, 1	-	-1, -1, -1, -1, 1	-1, 1, 1, -1, -1	1, -1, -1, -1, 1	1, 1, 1, 1, 1	-1, -1, -1, -1, -1	1, 1, -1, -1, 1	1, -1, -1, -1, 1	1, -1, 1, -1, 1	1, 1, 1, 1, 1	1, -1, -1, -1, 1	1, 1, 1, 1, 1	1, 1, 1, 1, 1	1, -1, -1, -1, -1
RANK-IQA	1, -1, 1, 1, 1	1, 1, 1, 1, -1	-	-1, 1, 1, 1, -1	1, 1, 1, 1, 1	1, 1, 1, 1, 1	-1, 1, 1, 1, -1	1, 1, 1, 1, 1	1, -1, 1, 1, 1	1, 1, 1, 1, 1	1, 1, 1, 1, 1	1, 1, 1, 1, 1	1, 1, 1, 1, 1	1, 1, 1, 1, 1	-1, 1, 1, -1, 1
HYPER-IQA	1, -1, -1, -1, 1	1, -1, -1, 1, 1	1, -1, -1, -1, -1	-	1, -1, -1, -1, 1	1, 1, 1, 1, 1	-1, -1, -1, 1, -1	1, -1, -1, -1, 1	1, -1, -1, -1, 1	1, -1, -1, -1, 1	1, 1, 1, 1, 1	1, -1, -1, -1, 1	1, 1, 1, 1, 1	1, -1, -1, -1, 1	1, -1, -1, -1, -1
KONCEPT	-1, -1, -1, 1, -1	-1, -1, -1, 1, -1	-1, -1, -1, -1, -1	-1, -1, -1, 1, -1	-	1, 1, 1, 1, 1	-1, -1, -1, 1, -1	-1, -1, -1, 1, -1	-1, -1, -1, 1, -1	-1, -1, -1, 1, 1	-1, -1, -1, 1, 1	-1, -1, -1, -1, 1	-1, -1, -1, 1, 1	-1, -1, -1, 1, 1	-1, -1, -1, -1, -1
FPR	-1, -1, -1, -1, -1	-1, -1, -1, -1, -1	-1, -1, -1, -1, -1	-1, -1, -1, -1, -1	-1, -1, -1, -1, -1	-	-1, -1, -1, -1, -1	-1, -1, -1, -1, -1	-1, -1, -1, -1, -1	-1, -1, -1, -1, -1	-1, -1, -1, -1, -1	-1, -1, -1, -1, -1	-1, -1, -1, -1, -1	-1, -1, -1, -1, -1	-1, -1, -1, -1, -1
NIMA	1, -1, -1, -1, 1	1, 1, -1, -1, 1	1, -1, -1, -1, 1	1, 1, 1, -1, -1	1, 1, 1, -1, 1	1, 1, 1, 1, 1	-1, -1, -1, -1, -1	1, 1, -1, -1, 1	1, -1, -1, -1, 1	1, 1, 1, -1, 1	1, 1, 1, 1, 1	1, 1, 1, -1, 1	1, 1, 1, -1, 1	1, 1, 1, -1, 1	-1, 1, -1, -1, -1
WSP	-1, -1, -1, 1, 1	-1, -1, 1, 1, -1	-1, -1, -1, -1, -1	-1, 1, 1, 1, -1	-1, -1, 1, -1, 1	1, 1, 1, 1, 1	-1, -1, 1, 1, -1	-	-1, -1, -1, 1, -1	1, -1, 1, 1, 1	1, 1, 1, 1, 1	1, -1, -1, -1, 1	1, 1, 1, 1, 1	1, 1, 1, -1, 1	-1, 1, -1, -1, -1
MDTVSFA	-1, -1, -1, -1, 1	-1, -1, -1, 1, -1	-1, -1, -1, -1, -1	-1, 1, 1, -1, -1	1, 1, 1, -1, 1	1, 1, 1, 1, 1	-1, 1, 1, 1, -1	1, 1, 1, -1, -1	-	1, 1, 1, -1, 1	1, 1, 1, 1, 1	1, 1, 1, -1, 1	1, 1, 1, -1, 1	1, 1, 1, -1, 1	-1, 1, 1, -1, -1
LINEARITY	-1, -1, -1, -1, -1	-1, 1, -1, 1, -1	-1, -1, -1, -1, -1	-1, 1, 1, 1, -1	-1, -1, -1, -1, -1	1, 1, 1, 1, 1	-1, -1, -1, 1, -1	-1, -1, -1, -1, -1	-1, -1, -1, 1, -1	-1, -1, -1, -1, -1	1, 1, 1, 1, -1	-1, -1, -1, -1, -1	-1, 1, 1, -1, -1	-1, 1, 1, -1, -1	-1, 1, -1, -1, -1
VSFA	-1, -1, -1, -1, -1	-1, -1, -1, -1, -1	-1, -1, -1, -1, -1	-1, -1, -1, -1, -1	-1, -1, -1, -1, -1	1, 1, 1, 1, 1	-1, -1, -1, -1, -1	-1, -1, -1, -1, -1	-1, -1, -1, -1, -1	-1, -1, -1, -1, -1	-	-1, -1, -1, -1, -1	-1, -1, -1, -1, -1	-1, -1, -1, -1, -1	-1, -1, -1, -1, -1
PAQ2PIQ	-1, -1, -1, 1, -1	-1, 1, 1, 1, -1	-1, -1, -1, -1, -1	-1, 1, 1, 1, -1	-1, 1, 1, 1, -1	1, 1, 1, 1, 1	-1, -1, 1, 1, -1	-1, 1, -1, 1, -1	-1, -1, -1, 1, -1	1, 1, 1, 1, 1	1, 1, 1, 1, 1	-	1, 1, 1, 1, -1	-1, 1, 1, -1, -1	-1, 1, -1, 1, -1
SPAQ	-1, -1, -1, -1, -1	-1, -1, -1, 1, -1	-1, -1, -1, -1, -1	-1, 1, 1, 1, -1	-1, -1, -1, -1, -1	1, 1, 1, 1, 1	-1, -1, -1, 1, -1	-1, -1, -1, -1, -1	-1, -1, -1, 1, -1	1, -1, -1, 1, 1	1, 1, 1, 1, 1	-1, -1, -1, -1, 1	-	-1, -1, -1, -1, -1	-1, 1, -1, -1, -1
TRES	-1, -1, -1, 1, -1	-1, 1, -1, 1, -1	-1, -1, -1, -1, -1	-1, 1, 1, 1, -1	-1, -1, -1, -1, -1	1, 1, 1, 1, 1	-1, -1, -1, 1, -1	-1, 1, -1, 1, -1	-1, -1, -1, 1, -1	1, -1, 1, 1, 1	1, 1, 1, 1, 1	1, -1, -1, -1, 1	1, 1, 1, 1, 1	-	-1, 1, -1, -1, -1
MANIQA	1, -1, -1, 1, 1	1, -1, 1, 1, 1	1, -1, -1, -1, 1	1, 1, 1, 1, 1	1, -1, 1, -1, 1	1, 1, 1, 1, 1	1, -1, 1, 1, 1	1, -1, 1, 1, 1	1, -1, -1, 1, 1	1, -1, 1, 1, 1	1, 1, 1, 1, 1	1, -1, 1, -1, 1	1, 1, 1, 1, 1	1, -1, 1, 1, 1	-

Table 16: Results of one-sided Wilcoxon rank-sum tests performed on Absolute gains for the metrics compared above. For each pair of metrics, the table shows values for different types of attacks in the following order: all attacks, FGSM-based, Korhonen-et-al, MADC, UAP-based. A value of 1 indicates the metric for that row is statistically superior to the metric for that column (its gains are lower than the gains of the metric in the column). A -1 value indicates the opposite. A hyphen (-) indicates they cannot be statistically distinguished with p-value  $\leq 0.05$ .